PROCEEDINGS
OF THE
CALIFORNIA ACADEMY OF SCIENCES
FOURTH SERIES

Vol. XXXIII, No. 12, pp. 361–414; 24 figs.; 5 tables May 12, 1966

GEOLOGY OF THE ISLAS REVILLAGIGEDO, MEXICO, 2. GEOLOGY AND PETROGRAPHY OF ISLA SAN BENEDICTO[1,2]

By

Adrian F. Richards

United States Navy Electronics Laboratory, San Diego, California[3]

Abstract: Isla San Benedicto is located where the Clarion fracture zone crosses a range of submarine volcanoes extending south towards Clipperton Island and including Isla Socorro. Field work conducted from 1952 to 1957 shows that San Benedicto is situated at the intersection of four local submarine ridges thought to mark fissures; the one extending north is the longest. Compared to the other three islands in the Revillagigedo archipelago, the insular shelf of San Benedicto is poorly developed and very narrow; shelf-break occurs at 55 to 75 fathoms. Principal landforms are large eroded trachytic domes, older in age than late Pleistocene, and two pyroclastic volcanoes of recent origin. The first geological map of the island shows that by volume the most abundant rock above sea level is sodic trachyte. Flows of trachybasalt and trachyandesite (mugearite) occur in a low stratigraphic position on the island and trachybasalt has been dredged from the narrow ridge extending north of the island. Accessory sodic rhyolite blocks were ejected from Volcán Bárcena during the eruption of August, 1952, to March, 1953. Twelve new chemical and 16 new alkali analyses of San Benedicto rocks indicate a reasonably regular differentiation from trachybasalt (alkali basalt) to sodic rhyolite, and an alkali-lime index of 52.6. Tholeiitic basalts, high alumina basalts, and rocks bearing feldspathoids have not been found. The increasing age and the decreasing quantity of silicic lavas and active volcanism from east to west in the Revillagigedos appears related to convection under the East Pacific Rise. The relationship to the Rise appears to account for the similarity of sodic rhyolites found on San Benedicto, Socorro, Easter Island, and elsewhere in the Pacific basin.

[1] References to numbers 1, 3, and 4 of this series are cited in the bibliography in the present paper.

[2] Contribution from the Scripps Institution of Oceanography, University of California, New Series.

[3] Present address, Departments of Geology and Civil Engineering, University of Illinois, Urbana, Illinois 61803.

CONTENTS

INTRODUCTION

Isla San Benedicto is the third largest and most northeasterly of the four Islas Revillagigedo. It is located about 870 nautical miles south-southeast of San Diego, California (fig. 1); 220 miles south of Cabo San Lucas, the south tip of Baja California; and in the same latitude as Colima, Parícutin, Popocatépetl, and other volcanoes of the trans-Mexico volcanic axis.

On August 1, 1952, San Benedicto literally burst from obscurity to become known as the location of the first new volcano in the east Pacific Ocean whose birth was observed by human eyes. The birth and development of Volcán Bárcena, as the new volcano was named, is described in detail elsewhere (Richards, 1959—hereafter called part 1). Studies of this volcano led to an investigation of the terrestrial and submarine geology of the Revillagigedo archipelago by the University of California's Scripps Institution of Oceanography, in part with the cooperation of the Instituto de Geofísica, Universidad Nacional de México, and with the assistance of investigators from other institutions and organizations in the United States and Mexico.

San Benedicto was discovered by the Spanish explorer Ruy López de Villalobos in 1542. According to Herrera (Burney, 1803, p. 226–232), López de Villalobos named the island Santo Tomé. Other historians claim he called it Anublada or Nublada, meaning cloudy. A discussion of the early names applied to the island is given by Richards and Brattstrom (1959). The island never has been inhabited.

The first landing and geological study of San Benedicto was made on December 25, 1862, by members of the Longinos Banda expedition. Banda (1862, p. 183–184) reported that the island was volcanic, but not of recent origin, and that the rocks included basalt, trachyte, porphry, and pumice. There were brief visits to this island by expeditions of the California Academy of Sciences in 1905 (Slevin, 1931) and 1925 (Hanna, 1926), but if specimens were collected they are not known to be extant (L. G. Hertlein, personal communication).

Robert S. Dietz conducted the first investigation of the new volcano on two U.S. Air Force flights to the island in September, 1952, (Dietz, 1953). Howel Williams prepared a geological sketch map of San Benedicto during the time the plane circled the island on the second flight. In addition to papers listed in Richards and Brattstrom (1959) that briefly describe aspects of the eruption of Volcán Bárcena, more recent reports have appeared by Maldonado-Koerdell (1958b), Mooser (1958), Richards (1960), and Brattstrom (1963).

Field work consisted of a short visit by private ship in 1952 and by research ships of the Scripps Institution in 1953, 1955 (two cruises), and 1957. Ten photographic and observation flights were made to the island between early September, 1952, and late January, 1956, (part 1; Richards and Brattstrom, 1959); an additional flight was made in 1961. North of Cráter Herrera (fig. 2)

FIGURE 1. Location of the Islas Revillagigedo.

the geology was largely investigated by observing and sampling the near-vertical cliffs, and was appreciably assisted by examination of stereo-oblique air photographs taken at close range during an encirclement of the island by an airplane flying at an altitude of 600 feet. Elsewhere, investigations were conducted on

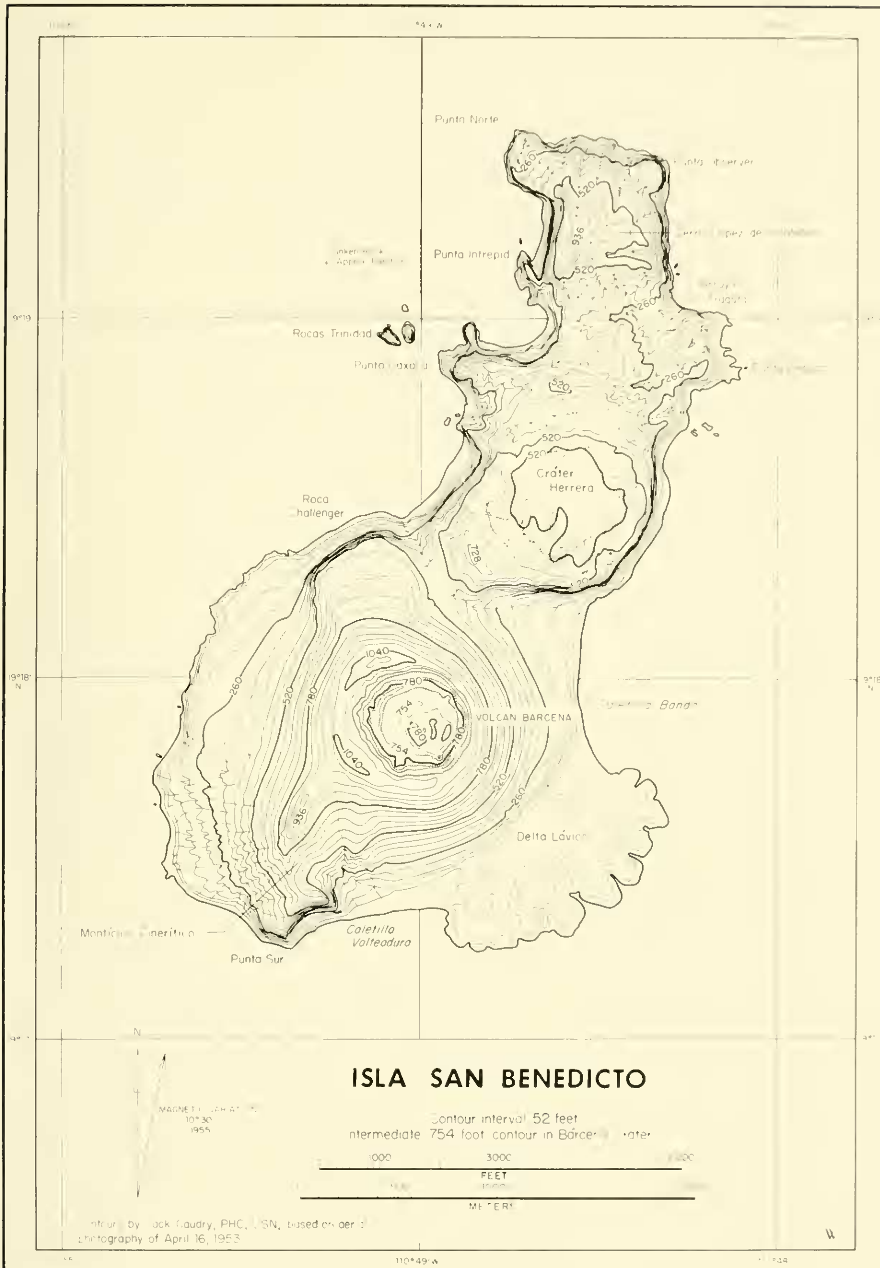

FIGURE 2. Topographic map of Isla San Benedicto.

foot with the aid of numerous photographs taken from airplanes, ships, and on land. Bathymetric studies in the vicinity of San Benedicto were made using techniques stated in the appendix; soundings in this region prior to 1952 were almost nonexistent.

It is possible to land on San Benedicto with impunity using a row boat only immediately adjacent to the Delta Lávico (usually west of the flow because of the prevailing northerly seas) or on the small pocket beach north of the prominent dikes at Punta Ortolan.

ACKNOWLEDGMENTS

In addition to those persons and organizations acknowledged in part one, Drs. Cordell Durrell and Howel Williams are thanked for petrographic assistance and for helpful discussions on different phases of the investigation. Dr. Williams also contributed a chemical analysis of a piece of floating pumice. Dr. Edward J. Zeller made available the alkali analyses. The two chemical analyses of submarine lava were financed by the California Research Corporation and made available by Drs. Jack Green and N. Allen Riley. Other chemical analyses, some film, and certain travel expenses were financed by Geological Society of America Project Grant 625–53. This paper was revised from part of my doctoral dissertation during the winter of 1960–1961, when I was a National Academy of Sciences—National Research Council Post-doctoral Resident Research Associate at the U.S. Navy Electronics Laboratory working under Dr. E. L. Hamilton. Additional changes to the manuscript were made in January, 1965, at the University of Illinois. I am appreciative to Drs. W. Bryan, Jr., G. Macdonald, and S. R. Nockolds and Ings. F. Mooser and G. P. Salas for reviewing a preliminary copy of this paper and for making helpful suggestions. Opinions and assertions in this paper are my own and are not to be construed as official views of organizations within the Department of Navy.

GEOLOGIC SETTING

Regional.

In the early 19th century Humboldt (1811, p. 221) supposed ". . . that there exists in this part of Mexico (region of Volcán Jorullo), at a great depth in the interior of the earth, a chasm in a direction from east to west—from the Gulf of Mexico to the South Sea." He wondered if the "chasm" extended to the Islas Revillagigedo, which are in the same latitude as the trans-Mexico volcanoes. More recently Menard (1955, p. 1167–1170) proposed that the submergent features of the Clarion fracture zone, extending over 2000 nautical miles west of Isla Clarión, are related to the Islas Revillagigedo and the trans-Mexico volcanic belt. This belt is characterized by late Cenozoic and Recent volcanoes (de Cserna, 1958); recent tectonic interpretations have been made by Maldonado-Koerdell (1958a) and by Mooser and Maldonado-Koerdell (1961). Menard believed that the most probable age of this and other fracture zones off North America was post Mesozoic.

The Clarion fracture zone has been explored in some detail from 121° W. to 109° W. West of 116° W. it is characterized by a narrow, east west trending ridge located in 18° 10′ N. latitude at the south side of the fracture zone. A trough extends parellel to and is located north of the ridge. Between Clarión and Socorro the ridge is discontinuous. There is some bathymetric evidence indicating that it may continue from about 111° W. (the longitude of Socorro) to about 110° W.; over this distance it is broader and located about 18° N. If this evidence is valid, it is possible that the apparent 10-nautical-mile displacement is related to the range of submarine volcanoes extending over 300 nautical miles south of Socorro toward Clipperton Island (Richards, 1957a, 1957b). Just north of Clipperton this range is represented by the Mathematicians Seamounts (see Menard and Fisher, 1958). Isla San Benedicto is located at the north end of the same range. The Revillagigedo archipelago is located on the west flank of the East Pacific Rise (see Menard, 1958; 1959, p. 207; 1960).

Isla Clarión appears to be genetically related to the Clarion fracture zone and the oldest island in the archipelago for the following reasons: (1) there is an east–west elongation of the deep submarine isobaths around the island, (2) the oldest rocks on land were erupted from an east–west fissure extending along the south side of Clarión (Bryan, 1959), and (3) Clarión has, compared to the other islands, more advanced terrestrial erosion, (4) a greater insular shelf width, (5) better development of fringing coral reefs, and (6) no historic record of volcanic activity.

The relative age of Isla Roca Partida is uncertain (Richards, 1964). If a west to east progression of volcanism occurred in the Islas Revillagigedo similar to the Hawaiian, Caroline, and Society islands (Richards and Dietz, 1956, p. 165), then Roca Partida is probably younger than Clarión but older than San Benedicto and Socorro, which probably are about the same age.

There is no historic record of volcanic activity on San Benedicto before the eruption of Bárcena in 1952. Socorro is the only island in the archipelago with known past activity, reported eruptions having occurred in 1848 (Revere, 1849, see reprint, 1947, p. 234–235), 1896 (Yarza, 1948, p. 163), and 1951 (Crowe and Crowe, 1955, p. 252). Sapper (1917a, p. 299) cites a manuscript by Noak stating that floating pumice, presumably from a submarine volcano, was reported in the vicinity of the Revillagigedos, 19° N. and 110° 12′ W.; unfortunately, a date was not given by Noak. A misprint of the longitude is given in another paper by Sapper (1917b, p. 75), which is repeated by Neumann van Padang (1938, p. 95). There is no bathymetric evidence for a submarine volcano in this location and it is likely that the observed pumice had a terrestrial origin, conceivably from the Montículo Cinerítico volcano on San Benedicto? Large amounts of drift pumice similarly resulted from the eruption of Volcán Bárcena (Richards, 1958a). Detected earthquakes reported by the United States Coast and Geodetic Survey are rare in the vicinity of the Islas Revillagigedo. In the period 1952 through 1959, 7 earthquakes were reported, 5 of which appear to have had epicenters near Isla San Benedicto and Isla Socorro.

Local.

Orientation of four submarine ridges at San Benedicto suggests the probable presence of a major fissure striking about N. 15° to 20° W. and two minor fissures striking about N. 37° E. and N. 41° W. (fig. 3). A 3-mile strike-slip displacement of the major ridge (N. 15° to 20° W.) by the one extending southwest of the island may have occurred, but the evidence is inconclusive. The fissures intersect at Isla San Benedicto, which represents the location of the maximum outpouring of lava. In figure 3, the dashed lines represent the inferred continuation of fissures for which there is no bathymetric evidence.

Where the topography is not complicated by ridges, the insular slope between 100 and 500 fathoms is about 20°. An abrupt change of declivity, the shelf-break, is located between insular slope and shelf. Off south San Benedicto shelf-break occurs at 55 to 60 fathoms near the Delta Lávico. Off north San Benedicto a shelf-break of about 70 to 75 fathoms was recorded on a line of soundings north-northeast of Punta Observer. Elsewhere, shelf-break is poorly defined on echograms. According to the concept of Dietz and Menard (1951, p. 2011), shelf-break is abrasional in origin and related to sea level about 5 fathoms or less above the break. This implies that the shelf was cut during a lower sea level, presumably during the Pleistocene. An alternative explanation, that the island has submerged this much, is unlikely. The gradually decreasing depth of shelf-break from north to south suggests tilt of the insular mass, probably caused by ascending magma under the south part of the island. The insular shelf is absent southwest of Montículo Cinerítico, which apparently extends across it. In the vicinity of Cráter Herrera the shelf is about 3800 feet wide. The shelf is the broadest off Cerro López de Villalobos, where it extends 3300 to 9000 feet beyond the shoreline. In this region it has a seaward slope of 3° to 8°.

CARTOGRAPHY

The first map of Isla San Benedicto probably was drawn by Captain Colnett, R. N., (1798) in 1793. A sketch survey made by the officers and men under Commander George Dewey of the U.S.S. *Narragansett* in 1874 was the first map to show the island in any detail. This sketch was in use on U.S. Navy Hydrographic Office chart no. 1688 as recently as the edition of 1951.

San Benedicto was photographed from the air in April and May, 1953, by the U.S. Navy Photographic Squadron Sixty-one at the request of the Office of Naval Research for the Scripps Institution of Oceanography. Jack Caudry,

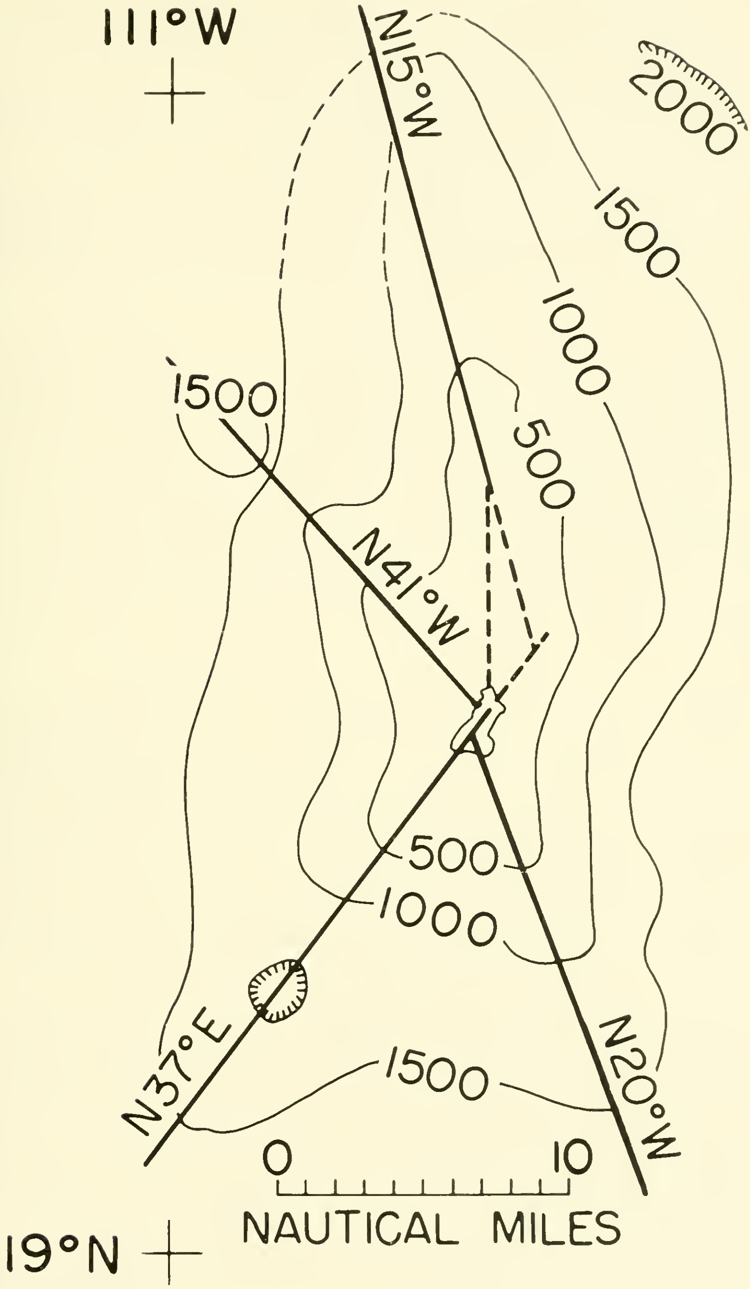

Figure 3. Map showing the inferred submarine fissure pattern in the vicinity of San Benedicto.

PHC, USN, prepared an excellent topographic map from these photographs during the summer of 1954. He drew form lines by stereocomparagraph and multiplex methods from the aerial photographs taken on April 16, 1953. Technical assumptions made by me when the contour interval, geographic coordinates, and scale were established are discussed in the appendix.

This new map (fig. 4 and fig. 2) shows that San Benedicto is about 2.8 miles long, 1.6 miles wide at Volcán Bárcena, and has an area of 2.32 square statute miles. Geographic names shown on this map previously were reported and discussed by Richards and Brattstrom (1959).

GEOLOGY

San Benedicto is divided into four regions for descriptive purposes: the long submarine ridge extending north of the island; a region of eroded domes, lava flows, and tuffs extending from Cráter Herrera to the north end of the island and including the Rocas Trinidad sea stacks; Roca Challenger and Cráter Herrera domes; and the tephra (collective term for all rock materials fragmented by a volcanic eruption that have not consolidated) cones of Bárcena and Montículo Cinerítico and their associated lava flows. The west side of the island is not easily accessible and is less well known compared to the east side, particularly north of Cráter Herrera.

North ridge.

It seems appropriate to call the long, narrow submarine ridge extending almost due north of Isla San Benedicto (fig. 5) "North Ridge" because of its lineation. Bathymetry of the north part of this ridge is only approximately defined in figure 5 because of the difficulty in obtaining accurate bearings on the island. The extreme north end is abruptly terminated about 23 nautical miles north-northwest of San Benedicto by a moat. The narrowness of the ridge is indicated by a 5.5-mile width between 1000-fathom isobaths 10 miles north of the island and a 4-mile width 15 miles north. Less than 7 miles north of San Benedicto the ridge changes direction from north to north-northwest.

A number of shoal areas, not all of which are shown in figure 5 because of the scale, are located on North Ridge. Possibly these areas may represent parasitic cones or domes? It is equally possible that the "cones" will be found to coalese and become north–south ridges when North Ridge is surveyed in greater detail. The shoal areas have an average slope of 13° to 24° in the upper 150 to 200 fathoms, generally steeper than the 15° flank slope normal to the ridge axis 10 miles north of the island.

Olivine-bearing alkali basalt lava and scoria was dredged from a depth of about 350 fathoms near the summit of North Ridge at a distance of 8 nautical miles from the island in March, 1957. It is likely that the bulk of North Ridge is composed of tephra and lava having about this composition.

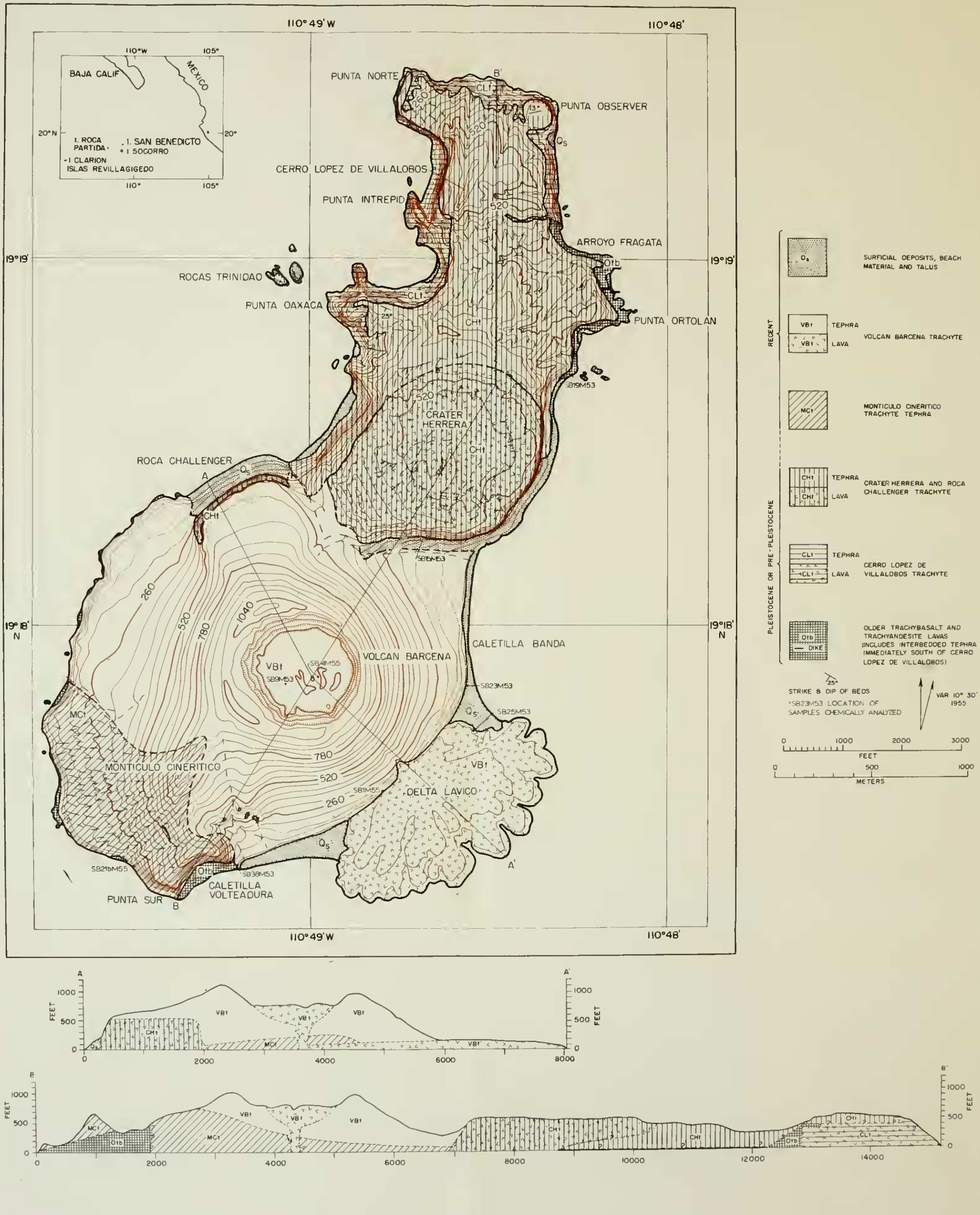

FIGURE 4. Geologic Map of Isla San Benedicto.

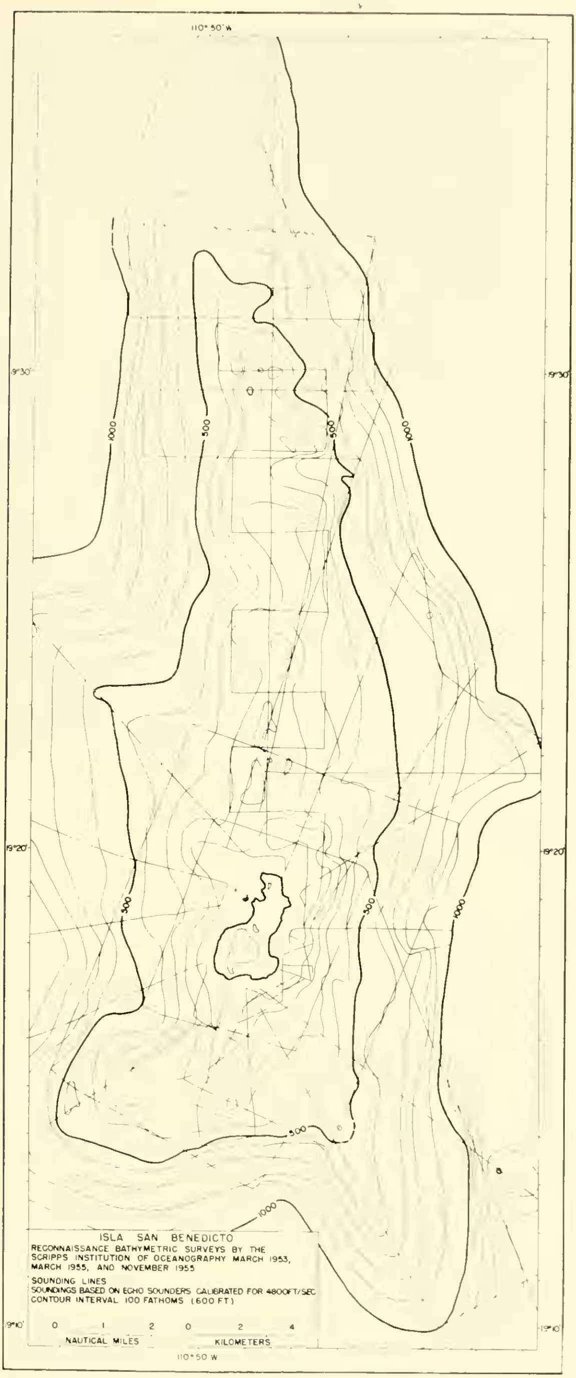

Figure 5. Map of the submarine topography in the vicinity of Isla San Benedicto.

Figure 6. Oblique air photograph of the north side of San Benedicto showing tuffaceous strata dipping north. Punta Observer just to left of photograph, Rocas Trinidad top center. U.S. Navy official photo, November 15, 1952.

North end of Isla San Benedicto.

North of Cráter Herrera the island consists of mafic flows occurring near sea level; overlying trachytic tuffs, tephra, and lava; and the complex of Cerro López de Villalobos. Bárcena tephra covers most of the outcrops, except those in the arroyos, and the geology is best observed in the sea-cliffs (fig. 6).

Flows of trachybasalt extend from under the north end of Cráter Herrera to Cerro López de Villalobos. Most of Punta Ortolan is composed of these flows and tuffs. South of the point the flows are thin and are found at the base of the east sea-cliff. The least silicic lava thus far found on San Benedicto, trachybasalt, occurs as a conspicuous small flow of dense, dark gray lava with abundant reddish-brown olivine megaphenocrysts just north of the minor headland with off-lying rocks located about 1200 feet south of Punta Ortolan. The flows and tuffs comprising Punta Ortolan are capped with a flow of trachyandesite and are cut by vertical dikes both north and south of the point. North of the point these dikes are composed of trachyandesite and appear to intersect the horizontal

Figure 7. Oblique air photograph of the northeast end of San Benedicto. Punta Ortolan, vertical dikes (shown by arrows), and landing place to the right of arrows; Punta Observer extreme right. U.S. Navy official photo, May 27, 1955.

trachyandesite flow; they do not extend into the flow of trachyte directly above it. Commencing with the small promontory north of Punta Ortolan, interbedded tuffs and flows of trachybasalt and trachyandesite dipping about 30° south-southwest abut against the massive lava of the Cerro. They do not appear to be exposed on the west side of the island.

Thick deposits of horizontally-bedded trachytic tephra, tuff, and lava extending from under the dome of Cráter Herrera to the north end of the island cover the more basic flows. South of the Cerro, these deposits and overlying Bárcena tephra are dissected by the Arroyo Fragata drainage system. The prominent ridge paralleling Cráter Herrera to the north appears from the east cliff exposure to be composed of these tuffs, although trachytic lava crops out on the south side midway between shores.

Cerro López de Villalobos geology is relatively more complicated. The Cerro is veneered on the north side with trachyte and sodic andesite (?) tuffs and lavas that dip about 30° to the north (fig. 7). On the southeast side, as previously mentioned, mafic lavas and tuffs dip to the south-southwest. On the southwest side about 1000 feet south of Punta Intrepid, horizontally-bedded tuffaceous strata turn up where they abut against the massive lava of the Cerro. Punta Observer is composed of massive trachytic lava. Presumably the unsampled lava exposed in the east cliff of the Cerro is part of the same structure? Columnar

Figure 8. Photograph of Roca Challenger viewed from the east before the eruption of Volcán Bárcena. Cráter Herrera to right. D. H. Bates photo, February, 1952.

jointing is fairly well developed south of Punta Observer. A flow of trachyandesite having a slight dip to the east conspicuously crops out on the south flank of the Cerro at an altitude of about 260 feet. It does not appear to extend very far to the north. This flow and the massive trachytic lava farther north are overlain by nearly-horizontal trachytic tuffs and lavas.

Northwest of Cráter Herrera a lithic basaltic tuff is found at the foot of the arroyo immediately south of Punta Oaxaca. Elsewhere in this region the horizontal strata predominantly are trachytic tuffs. The massive lava of Punta Oaxaca is trachyte and the lithic trachytic tuffs overlying it dip about 25° to the south-southwest.

The relation of the remnants of the presumably trachytic domes of Punta Oaxaca, Rocas Trinidad, the sunken rock west of the Rocas Trinidad, and one or more domes of Cerro López de Villalobos is obscure. The extent of the insular shelf off the north end of the island suggests that long ago there may have been a number of volcanoes in this region.

Cráter Herrera and Roca Challenger.

The domes of Roca Challenger and Cráter Herrera are similar in appearance, structure, and composition. Both are steep-sided, nearly cylindrical in plan, rise over 500 feet above sea level, and have a rocky talus at their base. It is uncertain whether they interconnect beneath the pyroclastics that connect the two domes (see fig. 8). Roca Challenger has an approximate diameter of 2000 feet and an estimated volume of 700 to 1300 million cubic feet above sea level (estimate aided with pre-Bárcena photographs). Cráter Herrera has an average diameter of 3000 feet and an estimated volume above sea level of 1500 to 3500 million cubic feet. More exact volumetric figures cannot be obtained because

Figure 9. Oblique air photograph of Cráter Herrera showing summit crater, resistant outcrop on north rim (foreground), and Volcán Bárcena and Roca Challenger in background. Water is ponded in the north part of the crater. U.S. Navy official photo, September 21, 1953.

the position of contacts beneath the domes, except for a few places, are unknown.

The top of Roca Challenger was very slightly convex and littered with scattered angular blocks before the eruption of Bárcena (fig. 8). The top of Cráter Herrera still is basin-shaped, . . ."the most perfect crater many of us had seen" (Hanna, 1926, p. 63), and dips to the northeast (fig. 9). Near the center of the depression there is a small summit crater that is breached to the northwest. A semi-detached outcrop of lava looking like an eroded spine is located at the north end of the basin; it represents a more resistant portion of the steep north rim. Attitude of Cráter Herrera trachyte lava above the tuffaceous trachytic strata on the northeast side suggests that at least Herrera dome was formed within the crater of a pyroclastic cone, now almost entirely eroded away, rather than being the remnant of an extremely large viscous extrusion. Trachytic lava of both domes is porphyritic, dense, and probably was emplaced by exogenous growth by effusion from a summit crater. Such a crater has not been observed on Roca Challenger, however. Vertical columnar jointing is well developed on most of the cliffs.

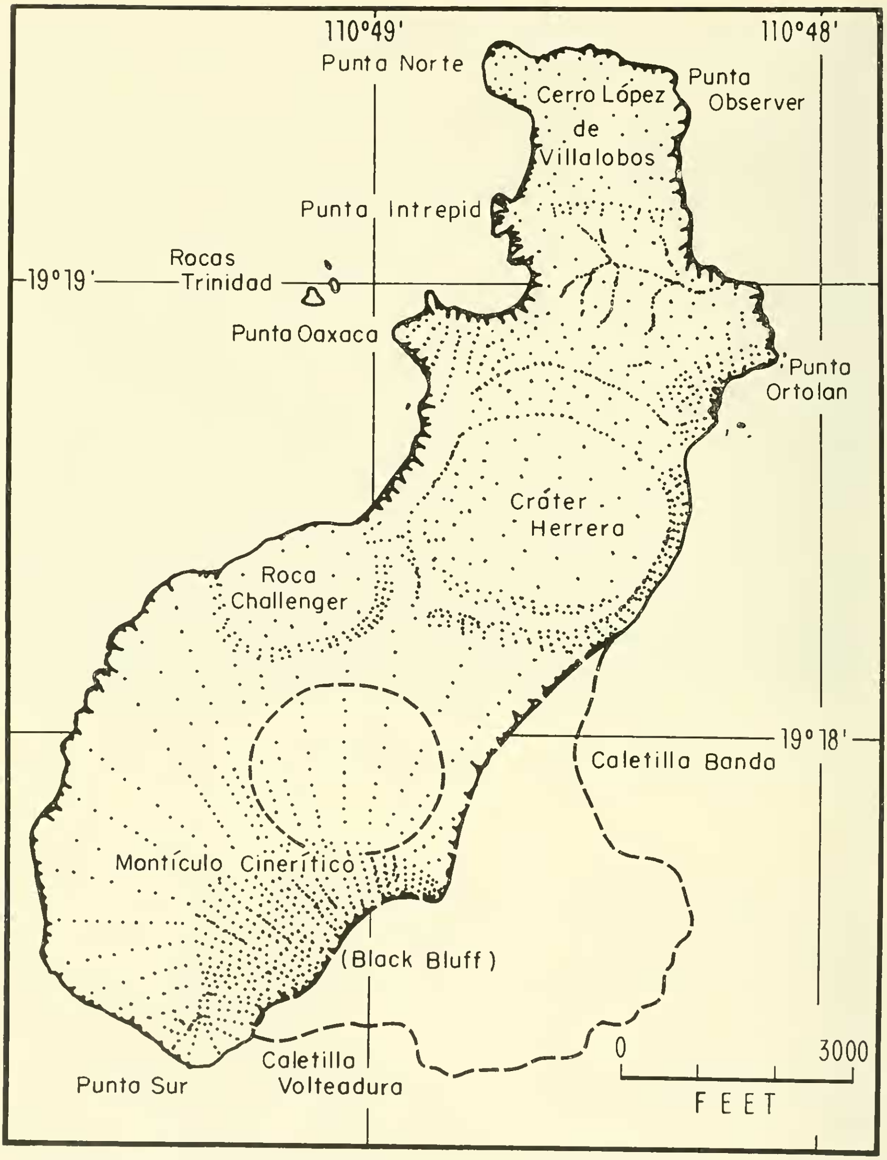

Figure 10. Sketch map showing the shoreline of Isla San Benedicto before the eruption of Volcán Bárcena in 1952.

Montículo Cinerítico.

Only the south and part of the west side of the remnant of a large, pluvially-dissected volcano called the Montículo Cinerítico (Ash Heap) escaped being buried by Bárcena tephra (fig. 10). The following description was possible only

Figure 11. Photograph of the Montículo Cinerítico tephra cone viewed from the east before the eruption of Volcán Bárcena. The vent is exposed showing vent agglomerate and a dome of trachytic lava partly filling the crater. D. H. Bates photo, February, 1952.

by a study of photographs taken in 1905 and 1925 by the California Academy of Sciences and in 1952 by Mr. D. H. Bates.

At the time Bárcena erupted, the east side of Volcán Cinerítico had been eroded away by waves exposing the vent, vent agglomerate, crater lava, and pyroclastic cone (fig. 11). Field inspection of the cone west of Punta Sur indicated that it is composed to trachytic ash, tuff, and beds of loose angular fragments of trachytic pumice. Only a very small portion of the crater lava escaped burial by Bárcena tephra; it crops out on the south flank of Bárcena (fig. 12).

The pre-Bárcena summit of Montículo Cinerítico had an altitude of 975 feet, according to U.S. Navy Hydrographic Office charts, and was the highest point on the island. The original diameter of the base of the volcano is estimated to be slightly greater than one mile and the crater rim probably had a diameter of about 3000 feet.

One or more trachyandesite lava flows having a thickness of 50 to 100 feet above sea level stratigraphically underlie Montículo Cinerítico pyroclastics and form the prominent sea-cliff on the southwest side of the island (fig. 13). Basalt or trachyandesite flows crop out in the southeast-facing, near vertical cliff of Montículo Cinerítico, slightly west and above the exposure of Montículo Cinerítico crater lava; and at the base of the southeast cliffs between Volteadura Beach and Punta Sur (fig. 12). These flows appear to be the eroded remains of an ancient volcano underlying the Montículo Cinerítico; they may be genetically related to the flows of similar composition located north of Cráter Herrera?

FIGURE 12. Photograph of the southeast face of Montículo Cinerítico showing outcrops of basalt and trachyandesite underlying Montículo Cinerítico tephra and partly covered by Bárcena tephra. A. F. Richards photo, March, 1953.

VOLCÁN BÁRCENA.

The birth and development of Bárcena and the subsequent effects of terrestrial and marine erosion of the volcano and Isla San Benedicto have been recorded in detail (part 1; Richards, 1965) and need not be repeated here.

Bárcena tephra cone initially had a maximum altitude of about 1120 feet, an exterior slope of 33°, and a 7° crater-rim slope to the east. The tephra is trachytic, having nearly the same chemical and mineralogical composition as the Montículo Cinerítico pyroclastics.

Two domes of trachytic lava are superposed, one above the other, in Bárcena crater (fig. 14). Both have central summit craters. Growth probably was largely by exogenous effusion, although it is not known for certain (part 1, p. 116). Later lava extrusion through the base of the cone resulted in magma withdrawal, subsidence of the domes, and fragmentation of their surface; the chilled margin of the outer, larger dome was left with relatively high relief. Subsequent rain erosion of the interior crater wall and redeposition on the floor of the crater is filling in low areas of the basined domes.

Bárcena first erupted on August 1, 1952. Initial activity was violent and cone growth was rapid. By August 12 the tephra cone was nearly fully formed

Figure 13. Oblique air photograph of the south side of San Benedicto showing the remnant of Montículo Cinerítico, Volcán Bárcena, and the Delta Lávico. U.S. Navy official photo, May 27, 1956.

Figure 14. Oblique air photograph of Bárcena crater showing encroachment of redeposited crater-wall material on the surface of the domes. Cráter Herrera and Cerro López de Villalobos in background. U. S. Navy official photo, May 27, 1955.

by fallout and by deposition from tephra avalanches (*nuées ardentes*). Cone formation ceased by mid-September. The domes were emplaced in November and early December. Lava began flowing out to sea from a basal fissure in the cone on December 8, continued until the end of February, 1953, and formed a large delta of lava—the Delta Lávico (fig. 15). Visible activity stopped at the end of February, except for quiet solfataric steaming from the lava flows.

In May, 1955, a bathymetric survey near the Delta Lávico was made to determine the submarine extent and underwater slope of a viscous flow of trachyte. The survey consisted of a pattern of 8 sounding lines approximately normal to the front of the flow and 3 to 4 lines, depending on the region, parallel to the margin. Soundings taken in March and November, 1953, were added to the map shown in figure 16, which originally was plotted to a scale of 1:5100.

A marked increase in declivity near the Delta Lávico is shown on echograms from sounding lines south of the flow. Lines southeast of the flow show less pronounced rises. Lines east and northeast did not show a change of slope as the margin of the flow was approached. It is inferred that the abrupt change of slope represents the submarine margin of the flow and the east and northeast lines did not reach the flow margin. The distance from the emergent edge of

Table 1. *Seaward slopes of the Delta Lávico.*

Terrestrial
December 10, 1952: 14°
March 9, 1953: 28° to 40°

Submarine

Sounding lines normal to flow	*Location off delta*	*Margin depth in feet*	*Distance of margin from shore in feet*	*Slope, to nearest half degree*
2	SSW	210	420	26.5
3	S	240	480	26.5
4	SSE	300*	660	24.5
5	SE	150*	405	20.5

* Approximate depth at change of declivity.

the delta to the submarine limit (fig. 16) averages 490 feet on the four lines that crossed the submarine portion of the flow (table 1). In December, 1952, the yacht *Observer* anchored in 120 to 126 feet of water 2700 feet from shore southeast of Bárcena (about 510 feet seaward of a line tangent to the edge of the flow tongues). The depth at this point still is about 120 feet, which is an additional indication that lava did not flow this far.

Submarine and terrestrial slopes determined from figure 16 and from visual observation, respectively, are listed in table 1. The pre-Delta Lávico submarine surface had an approximate slope of 3° to 7° to the southeast.

The bend seaward of the submarine isobaths southeast of the Delta Lávico probably is caused by a pre-Bárcena structure. Although the insular slope directly below the 300-foot shelf-break is about 33° (sonic soundings slope corrected from data by Raitt in Hamilton, 1956, fig. 12), the same as Bárcena cone, the similarity is coincidental; the 2700-foot distance from the seaward edge of the Delta Lávico and the presence of a shelf-break are evidence that the slope is not genetically related to Bárcena.

An area of irregular topography is located southwest of the Delta Lávico. The close proximity of two small peaks, rising within 60 feet of the surface, to Montículo Cinerítico and the hummocky topography in this area is suggestive that it may be related to the summit of an old volcano.

GEOLOGIC HISTORY

Rending of the sea floor by one or more fissures and the subsequent effusive outpouring of lava accompanied by explosive activity above a depth of about 1560 fathoms (equivalent to the critical pressure of sea water) gradually built a volcanic edifice rising more than 1800 fathoms or 11,000 feet above the ocean floor. Presumably this activity occurred in the late Cenozoic, although direct evidence is lacking.

FIGURE 15. Vertical air photograph of Isla San Benedicto taken from a 12,000 foot altitude before wave erosion attacked the Delta Lávico. U.S. Navy official photo, April 16, 1953.

The sequence of events resulting in the eruption of the mafic rocks of San Benedicto and their partial erosion by waves, rain, and wind, is obscure. There is some evidence for the existence of one or more large volcanoes in the general vicinity of Cerro López de Villalobos associated with the eruption of trachybasalts, trachyandesites, and a plug or plugs or trachyte. Conical geomorphic forms that are believed to be parasitic volcanoes are located below sea level north and south of the present island. They may have formed during Pleistocene lower stands of the sea or it is equally possible that they were submarine volcanoes at the time of their formation.

The size of Cráter Herrera and the thick deposits of pyroclastics underlying the dome to the north suggests that the tephra cone of Volcán Herrera was very large at the time that it was formed. Roca Challenger dome appears to have been closely associated with Volcán Herrera. The appearance of nearly all sides of Cráter Herrera and Roca Challenger indicates an extended period of wave erosion followed the cessation of Herrera activity; erosion completely wore away all sides of the cone except to the north and immediately adjacent to the southwest side of Cráter Herrera.

The extent of the insular shelf implies a pre- late-Pleistocene age for Volcán Herrera and those volcanoes formed before Herrera.

Montículo Cinerítico shows every sign of being relatively young. As speculated

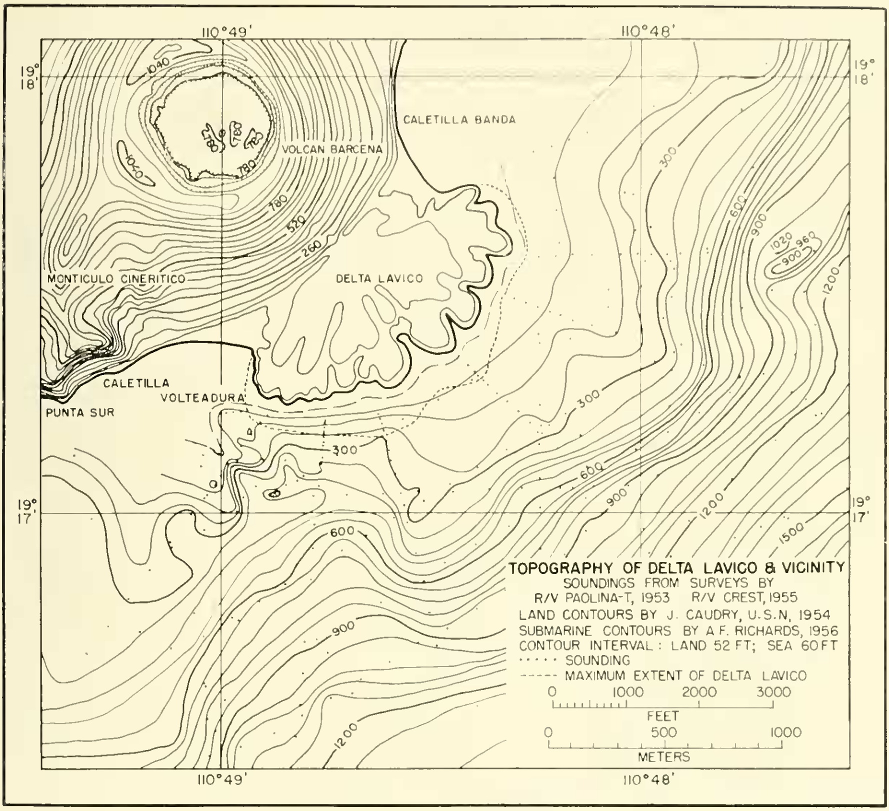

Figure 16. Map of the submarine topography in the vicinity of the Delta Lávico. Also shown is the probable maximum submarine extent of the lava flow.

previously, it may have erupted within the last few hundred years. Wave erosion had nearly carved the volcano in half by the time Volcán Bárcena was born in 1952.

Absence of fringing coral reefs around the island suggests that the eruption of Montículo Cinerítico and the subsequent erosion of its pumiceous cone liberated sufficient abrasive material into the surf zone to effectively inhibit the colonization of reef-forming corals at Isla San Benedicto.

PETROGRAHY

Seventy-five samples of San Benedicto lavas and pumices were examined in hand specimens, thin section, and by oil-immersion methods. Plagioclase composition was estimated from extinction angles (Winchell, 1951, p. 262, 283) and indices of refraction determined by immersion methods using data from Chayes (1952) and Crump and Ketner (1953, p. 31) given in Wahlstrom

(1955, p. 118). Where alkali feldspar composition is given it was estimated from optic axial angles and immersion in oil of n = 1.530 using graphs by Tuttle (1952) and modifications of these graphs by MacKenzie and Smith (1956). There is a marked difference in augite-aergirine composition determined by optic axial angles and extinction measurements in the rocks studied (see Tröger, 1952, p. 64, and *cf.* Winchell, 1951, p. 414). Consequently, molecular proportions are not assigned and the estimated optic axial angle and Z∧c extinction are stated. Olivine composition was obtained from estimated optic axial angles (Poldervaart, 1950, p. 1073). Rock color in hand specimens was determined from the rock color chart published by the Geological Society of America.

Most of the rocks examined in thin section are too fine-grained for modal analysis. Rocks for which chemical data are available are named in accordance with the chemical classification proposed by Rittmann (1952, 1960) for the *Catalogue of the Active Volcanoes of the World*. Where modes were determinable, nomenclature by Williams and others (1954) has been used, and is preferred where discrepancies exist between the two classifications.

Petrographic descriptions in this paper are generalized according to rock type, except for Bárcena tephra and lava which are described separately. Descriptions more directly related to specific locations on Isla San Benedicto are given elsewhere (Richards, 1957a).

Trachybasalts (Alkali Basalts).

The most mafic rock found on San Benedicto is a trachybasalt from northeast of Cráter Herrera. It is medium dark gray, vesicular, and porphyritic in hand specimen. In thin section, the lava consists of about 20 per cent phenocrysts of corroded, euhedral to anhedral calcic labradorite or bytownite ($An_{68 \text{ to } 76}$) that are up to 6 mm. in diameter and rimmed with andesine; rare, pale tanish-green, subhedral clear olivine; and more common embayed olivine ($Fo_{75 \text{ to } 80}$) showing alteration to iddingsite and opaques (20%); plagioclase microlites (40%), which appeared to be calcic andesine; and small, elongated, pale buff grains of augite (10%) having a +2V of about 40° and a Z∧c of 45°. Modal alkali feldspar was absent. The opaques are granular, although partly altered, yellowish red-brown, earthy microphenocrysts occur up to 0.3 mm. in size. Accessory apatite is rare. An alkalic content sufficiently high to warrant an alkali or trachy prefix was indicated by minute, elongated grains of a greenish-brown sodic amphibole (?) strongly pleochroic in shades of pale to dark grass green. A chemical analysis of this rock is given in table 4, no. 3.

Trachybasalts elsewhere are similar in composition, but usually contain only a few per cent of olivine, a little glass, and an occasional sanidine megaphenocryst. Olivines having the highest fosterite content occurred in submarine basalts from north of the island; a chemical analysis of a submarine basalt is given in table 4, nos. 1 and 2. In one basalt from under the Montículo Cinerítico.

a prismatic, subhedral augite microphenocryst was zoned and showed a Z∧c extinction of 47° in the core and about 58° in the rim, denoting a probable sodic enrichment of the melt. Most augites present in San Benedicto basalts and andesites have a +2V of about 50° and a Z∧c of about 50°, with slightly higher extinction angles occurring in groundmass augites.

Trachyandesites (Mugearites).

In hand specimen, San Benedicto trachyandesites (mugearites) range in color from dark brownish black to medium gray. They are usually vesicular and porphyritic, containing megaphenocrysts of plagioclase to 5 mm. in diameter, magnetite up to 8 mm., occasional alkali feldspar, and rare olivine to 1 mm. in diameter. Plagioclase phenocrysts in thin section, which show twinning according to the albite, carlsbad, and pericline laws, are composed of euhedral to subhedral corroded labradorite (An_{68}) that often show marginal resorption, and possess narrow, clear rims of oligoclase-andesine (about An_{30}). Olivines (about Fo_{75}) usually occur as microphenocrysts showing slight resorption and a little alteration; they are not common. Pale buff, subhedral augites (+2V 55° to 60° and Z∧c 50°) also occur as microphenocrysts.

An intergranular texture is most common. Oligoclase-andesine microphenocrysts and microlites comprise about 50 per cent of the rocks. Granular augite also occurs in the groundmass along with finely-divided opaques, some of which show alteration to an earthy, reddish oxide that may be goethite? Accessory acicular or granular apatite and interstitial glass are rare. The fine-grained dike north of Punta Ortolan shows a trachytic groundmass in which was found about 10 per cent modal alkali feldspar and a very small lath-shaped sodic amphibole (?). This mineral had low birefringence, moderate relief, a small extinction angle, and exhibited weak pleochroism in shades of yellow brown, pale reddish brown, and olive or greenish brown; it may be arfvedsonite or barkevikite?

One chemical analysis (table 4, no. 5) and two alkali analyses (table 5, columns A and B) of San Benedicto andesites show sufficient alkali to indicate that these andesites should be classified as trachyandesites or mugearites (Nockolds, 1954, p. 1018; Muir and Tilley, 1961); they all are of the oceanic type (see Macdonald, 1960).

Sodic trachytes.

San Benedicto trachytes in hand specimen range in color from medium gray to olive and brownish gray. Flows are usually vesicular while domes are not. Practically all trachytic pumices and lavas contain phenocrysts of blocky alkali feldspar and a small amount of sodic plagioclase up to 5 mm. in diameter, augite to 2 mm. long, and occasionally olivine. Cráter Herrera trachyte is typical of the group. A sample from the south cliff that was chemically analyzed (table 4, no. 9) contains megaphenocrysts of alkali feldspar (about 15%) and olivine (rare) set in a glassy trachytic groundmass of alkali feldspar microlites (70%), augite and aegirine-augite (about 7%), a few per cent each of opaques and interstitial quartz, and a little sodic amphibole and apatite. Phenocrysts of alkali feldspar are euhedral to subhedral and corroded, with common grid and very fine albite twinning. Remnants of the corroded interior and the rim have lower refractive indices than the central portion of a few phenocrysts, which indicates that apparently both the core and rim are more potassic than the central part. The transition from interior to central part of the crystals is abrupt and from the central part to the rim gradational. Sanidine (2V about 30°) and anorthoclase (2V 50–55°) are both present in separate phenocrysts. Olivines are iron-rich (greenish color), anhedral, and deeply embayed. Prismatic, subhedral, light-green augite (+2V 60°, Z∧c 50°) microphenocrysts show marginal alteration to a sodic amphibole having a very small extinction angle and strong pleochroism ($\alpha' =$ yellow brown and $\gamma' =$ very dark brown, almost black). The pleochroism suggests enigmatite (Bowen, 1937). This mineral also occurs in patches in the groundmass along with relatively abundant blunt-ended, rod-shaped aegirine-augite (Z∧c about 80°) possessing deep grass-green to brown pleochroism, and finely divided opaques that are probably magnetite. Alkali analyses of Cráter Herrera trachytes are listed in table 5, columns E and F.

Other trachytes may contain alkali feldspar phenocrysts having cross-hatch twinning (see MacKenzie, 1956), which probably is anorthoclase (2Z about 50°). Olivines (Fo_{55}) may have resorbed borders showing alteration to magnetite with a dark reddish-brown mineral (iddingsite?) at the margin. Tiny grains of a mineral having weak pleochroism in shades of yellowish pink and lemon also may be present in the groundmass. Alkali analyses of different trachytes are given in table 5, columns D–P.

SODIC RHYOLITES.

Although two analyzed pumices contain slightly more than 10 per cent normative quartz and are called sodic rhyolite, the only unequivocal rhyolites from San Benedicto are accessory blocks found lying on or near Bárcena cone. These blocks are up to a foot or more in diameter and apparently were blown out of the volcano during the last stages of the tephra eruption because they have not been found buried in the cone tephra. The blocks are subangular, mottled greenish gray and white in color, dense, and often show conspicuous flow structure. Phenocrysts of alkali feldspar, up to 3 mm. long, and rarely a green pyroxene, less than 2 mm. long, occur in hand specimen. In thin section, 5 to 10 percent of the rock consists of phenocrysts of subhedral sanidine having large cores with narrow rims of higher relief. Less common phenocryts of aegirine-augite (+2V about 70°) comprise about 10 per cent of the rock; they are 0.5 to 2 mm. long and show weak pleochroism in pale green, buff, and dark olive-green colors. The trachytic groundmass consists of about 50 per cent of microphenocrysts and microlites of alkali feldspar; 10 per cent of tiny laths and irregular patches of yellow-green to grass-green aegirine-augite (+2V 80°, ZΛc 85°); 2 per cent of riebeckite (?) having a small extinction angle and strongly pleochroic in shades of green, blue, and violet; and 3 per cent of a mineral exhibiting strong pleochroism in very dark brown- nearly opaque, pale yellow-brown, and reddish-brown colors, which may be enigmatite or cossyrite. Three to four per cent of opaques, some of which appear pseudomorphous after olivine, a very little accessory zircon, and about 5 per cent glass also were found in the groundmass. A quantitative determination of the interstitial quartz by X-ray diffraction was made by Dr. Robert Rex, who reported that one sample contained 8.7 ± 0.5 per cent quartz. Ten per cent was estimated in the thin section. This percentage indicates that the rocks are quartz trachytes according to Williams and others (1954, p. 98). Quartz in the norm (table 4, no. 12) however, is twice the amount in the mode and suggests that excess silica that might have crystallized as quartz may be contained in groundmass glass. A high temperature, primary origin of the free quartz is shown by an O^{18}/O^{16} ratio of 7.6 (sample SB1M55; R. Rex, personal communication). The rock is called a sodic rhyolite following Rittmann's classification, and because of the large amount of normative quartz. A chemical analysis is given in table 4, no. 12. An alkali analysis of another sample listed in table 5, column P, shows a Na_2O content higher by 1.4 per cent. These analyses show that the sodic rhyolite contains significantly higher Al_2O_3 and lower TiO_2 compared to pantellerites from Pantelleria (Washington, 1914, p. 17; Zies, 1960); consequently, they are not called pantellerite.

Volcán Bárcena.

Tephra. Examination of glass and phenocrysts in a specimen of black trachytic pumice from Bárcena cone and white pumices from Montículo Cinerítico shows a similar mineralogical composition (table 2). Bárcena pumice is less silicic, however, a fact indicated by the higher refractive index of Bárcena glass and by a chemical analysis (table 4). In Bárcena pumice, sanidine ($Or_{60}(Ab+An)_{40}$) is clear and subhedral; albite (An_4) is euhedral, cloudy, twinned according to the albite law, and possesses an intermediate 2V; and grass-green aegirine-augite ($N_y = 1.724$) is rod-shaped with lengths 3 to 8 times the width. An alkali analysis of another sample of Bárcena pumice is given in table 5, column 1. A chemical analysis of light-colored pumiceous ash is listed in column 8 of table 4; compare the alkali analysis of the same sample in table 5, column 4.

A large range is present in the refractive index of natural glass in several other Bárcena pumice samples (table 3). Glass of individual coarse ash particles has a constant refractive index. Variation appears to be present only between the glass of different ash particles, indicating a heterogeneous composition of the ashy tephra. Bárcena tephra may include both essential ash from Bárcena and

TABLE 2. *Refractive indices of phenocrysts and glass in San Benedicto pumices.*

Sample	Location	Glass refractive index (±0.002)	Sanidine refractive indices (±0.002)	Albite refractive indices (±0.002)	Aegirine-augite refractive indices (±0.006)
SB21M55	Montículo Cinerítico	1.503	N_x1.521		N_x1.727
			N_y1.527		N_y1.736
			N_z1.528		N_z1.756
SB21bM55	Montículo Cinerítico	1.503	1.521	N_x1.532	1.726
			1.527	N_y1.536	1.734
			1.528	N_z1.541	1.761
SB24M53	Bárcena	1.516	1.522	1.530	1.713
			1.527	1.534	1.724
			1.528	1.538	1.743

accessory ash from Montículo Cinerítico.

Bárcena lava ejected from the crater is a medium gray or black porphyritic trachyte. Some fragments are composed of over 50 per cent glass and have a subconchoidal fracture. Phenocrysts of sanidine, calcic oligoclase (about An_{25}), and a very little titaniferous augite are commonly set in a glassy groundmass of alkali feldspar, augite (+2V 60°, Z∧c 50°), granular opaques, and a very little accessory zircon. Needles of apatite are enclosed in alkali feldspar. A little olivine may be present. An alkali analysis is given in table 5, column J.

Lava. Six lava samples from the crater and eight from the Delta Lávico show essentially the same mineralogy. Petrographically all are oligoclase-augite andesites (mugearite) with one exception, which had sufficient modal alkali feldspar to be called a trachyte. A typical sample in hand specimen is vesicular, grayish black, and slightly porphyritic with occasional phenocrysts of blocky, lath-shaped alkali feldspar about 1 mm. long, augite up to 2 mm. long, olivine to 2 mm. long, and plagioclase, commonly 1 to 3 mm. in length—rarely to 13 mm. long.

In thin section, the groundmass texture is usually trachytic or felty. Sanidine phenocrysts are anhedral and corroded. Labradorite phenocrysts are euhedral to anhedral in lath and tabular shapes and are both corroded and clear. They are zoned from about An_{65} in the core to An_{28-30} in a narrow rim. Twinning is common. Calcic oligoclase also is found as microphenocrysts

TABLE 3. *Variation of glass refractive index in Bárcena pumices.*

Composite sample	Glass refractive index	Color of pumice	
SB23M53	1.506	white	
	1.510	gray	most common
	1.512	buff	most common
	1.523	black	

Table 4. *Chemical analyses.**

	1	*1b*	*2*	*2b*		*3*	
SiO_2	41.18	44.06	44.01	45.17	(21.10)	47.25	(22.09)
TiO_2	2.48	2.66	2.50	2.57	(1.54)	2.05	(1.23)
Al_2O_3	19.45	20.80	20.24	20.78	(10.98)	17.22	(9.11)
Fe_2O_3	6.05	6.47	3.89	3.99	(2.79)	5.05	(3.53)
FeO	4.06	4.34	4.85	4.98	(3.87)	5.26	(4.09)
MnO	0.08	0.09	0.09	0.09	(0.07)	0.14	(0.11)
MgO	4.48	4.79	4.02	4.13	(2.49)	6.10	(3.68)
CaO	9.66	10.34	11.30	11.60	(8.28)	9.72	(6.95)
Na_2O	3.39	3.63	3.39	3.48	(2.58)	3.34	(2.48)
K_2O	0.86	0.92	1.11	1.14	(0.95)	1.15	(0.95)
P_2O_5	1.73	1.85	1.81	1.86	(0.81)	0.32	(0.14)
H_2O^+	3.75	–	1.54	–	–	1.38	(0.15)
H_2O 110°C.	3.18	–	1.03	–	–	0.29	
CO_2	0.05	0.05	0.20	0.21	(0.06)	0.23	(0.06)
Cl	n.d.	n.d.	n.d.	n.d.		0.10	
F	n.d.	n.d.	n.d.	n.d.		n.d.	
	100.40	100.00	99.98	100.00		99.60	
–0 for Cl & F						0.02	
						99.58	

* Cation weight percentage in parenthesis follows the oxide weight percentage column for those analyses used in the variation diagrams.

Table 4. *Continued.*

	4		*5*		*6*		*7*	
SiO_2	48.28	(22.57)	54.94	(25.68)	60.78	(28.41)	61.33	(28.67)
TiO_2	2.64	(1.58)	1.58	(0.95)	0.73	(0.44)	0.76	(0.46)
Al_2O_3	19.09	(10.10)	17.07	(9.03)	16.11	(8.53)	16.82	(8.90)
Fe_2O_3	3.09	(2.16)	1.64	(1.15)	0.73	(0.51)	1.70	(1.19)
FeO	7.33	(5.70)	7.83	(6.09)	6.33	(4.92)	5.30	(4.12)
MnO	0.06	(0.05)	0.20	(0.15)	0.17	(0.13)	0.12	(0.09)
MgO	5.30	(3.20)	2.45	(1.48)	0.89	(0.54)	0.91	(0.55)
CaO	9.17	(6.55)	5.67	(4.05)	3.77	(2.69)	3.31	(2.37)
Na_2O	3.29	(2.44)	5.56	(4.13)	6.12	(4.54)	6.25	(4.64)
K_2O	0.92	(0.76)	2.30	(1.91)	3.20	(2.66)	3.18	(2.64)
P_2O_5	0.84	(0.37)	0.04	(0.02)	0.10	(0.04)	0.21	(0.09)
H_2O^+	0.00	(0.00)	0.60	(0.07)	0.43	(0.05)	0.44	(0.05)
H_2O^- 110°C.	0.00		0.11		0.04		0.01	
CO_2	0.00	(0.00)	0.00	(0.00)	0.00	(0.00)	0.00	(0.00)
Cl	n.d.		0.07		0.07		0.07	
F	n.d.		n.d.		n.d.		n.d.	
	100.01		100.06		99.47		100.41	
–0 for Cl &F			0.02		0.02		0.02	
			100.04		99.45		100.39	

TABLE 4. *Continued.*

	8a	8b		9		10a	10b	
SiO_2	61.66	64.60	(30.20)	64.19	(30.01)	62.49	67.45	(31.53)
TiO_2	0.47	0.49	(0.29)	0.38	(0.23)	0.28	0.30	(0.18)
Al_2O_3	15.27	16.00	(8.47)	16.42	(8.69)	14.36	15.51	(8.21)
Fe_2O_3	0.36	0.38	(0.25)	3.27	(2.29)	1.42	1.53	(1.07)
FeO	4.84	5.08	(3.95)	1.56	(1.21)	3.36	3.63	(2.82)
MnO	0.12	0.13	(0.10)	0.07	(0.05)	0.14	0.15	(0.12)
MgO	0.43	0.45	(0.27)	0.25	(0.15)	0.38	0.40	(0.24)
CaO	1.97	2.06	(1.47)	1.82	(1.30)	0.82	0.89	(0.64)
Na_2O	7.30	6.34	(4.70)	6.70	(4.97)	7.58	6.07	(4.50)
K_2O	4.25	4.46	(3.70)	4.53	(3.76)	3.61	3.90	(3.24)
P_2O_5	0.01	0.01	(0.00)	0.03	(0.01)	0.04	0.04	(0.02)
H_2O^+	2.12	–		0.42	(0.05)	2.13	–	
H_2O^- 110°C.	0.33	–		0.13		1.47*	–	
CO_2	0.00	0.00	(0.00)	0.00	(0.00)	nil	nil	(nil)
Cl	1.43	–		0.23		2.23	–	
F	n.d.	n.d.		n.d.		0.12	0.12	
	100.56	100.00		100.00		100.42	100.00	
–0 for Cl & F	0.31			0.05		0.55		
	100.25			99.95		99.87		

* 105°C.

TABLE 4. *Continued.*

	11a	11b		12	
SiO_2	64.91	68.44	(31.99)	69.90	(32.68)
TiO_2	0.26	0.27	(0.16)	0.17	(0.10)
Al_2O_3	13.83	14.59	(7.72)	13.96	(7.39)
Fe_2O_3	1.25	1.30	(0.91)	1.32	(0.92)
FeO	2.56	2.70	(2.10)	2.06	(1.60)
MnO	0.07	0.07	(0.05)	0.04	(0.03)
MgO	0.05	0.05	(0.03)	0.04	(0.02)
CaO	1.08	1.14	(0.81)	0.62	(0.44)
Na_2O	7.14	6.42	(4.76)	5.71	(4.24)
K_2O	4.72	4.98	(4.13)	4.65	(3.86)
P_2O_5	0.04	0.04	(0.02)	0.00	(0.00)
H_2O^+	2.20	–		0.58	(0.06)
H_2O 110°C.	0.52	–		0.05	
CO_2	0.00	0.00	(0.00)	0.00	(0.00)
Cl	1.21	–		0.29	
F	n.d.	n.d.		n.d.	
	99.84	100.00		99.39	
-0 for Cl & F	0.26			0.06	
	99.58			99.33	

Table 4. *Continued.*

C.I.P.W. Norms

(weight per cent)

	2b	3	4	5	6	7	8b	9	10b	11b	12
q	–	–	–	–	1.98	3.18	3.66	7.26	12.90	11.40	18.90
or	6.67	6.67	5.56	13.34	18.90	18.90	26.13	25.02	22.80	29.47	27.80
ab	28.30	28.30	27.77	46.63	51.87	52.40	53.45	55.54	51.35	47.16	46.63
an	37.81	29.75	34.47	15.57	7.51	8.62	2.22	3.06	3.61	–	–
ne	0.57	–	–	–	–	–	–	–	–	–	–
hl	–	0.35	–	0.23	0.23	0.23	–	0.77	–	–	0.94
ac	–	–	–	–	–	–	–	–	–	3.70	–
ns	–	–	–	–	–	–	–	–	–	0.61	–
wo	2.67	6.61	2.32	5.34	4.41	2.90	3.36	2.44	–	2.32	1.28
en	–	9.00	9.70	1.15	2.20	2.30	1.30	0.60	1.00	0.10	0.10
fs	–	1.32	5.02	2.04	10.30	7.26	8.45	–	5.15	4.62	2.51
fo	7.14	4.62	2.45	3.50	–	–	–	–	–	–	–
fa	1.22	0.82	1.32	6.94	–	–	–	–	–	–	–
mt	5.80	7.66	4.41	2.32	0.93	2.55	0.70	4.18	2.09	–	1.86
il	4.86	3.95	5.02	3.04	1.37	1.37	0.91	0.76	0.61	0.61	0.30
hm	–	–	–	–	–	–	–	0.48	–	–	–
ap	4.37	0.67	2.02	–	0.34	0.34	–	–	–	–	–
fr	–	–	–	–	–	–	–	–	0.47	–	–
cc	0.50	0.60	–	–	–	–	–	–	–	–	–
	99.91	100.32	100.06	100.10	100.04	100.05	100.18	100.11	99.98	99.99	100.32

Table 4. *Continued.*

1a. Trachybasalt. Analysis near the exterior (FIGURE 3). Dredged eight miles north of San Benedicto in 350 fathoms. H. B. Wiik, analyst.

1b. Trachybasalt. Analysis 1a computed water-free.

2a. Trachybasalt. Analysis near the center (FIGURE 3). Same specimen as 1a. H. B. Wiik, analyst.

2b. Trachybasalt. Analysis 2a computed water-free.

3. Trachybasalt (SB19M53). Lava from cove northeast of Cráter Herrera. H. B. Wiik, analyst.

4. Trachybasalt. Xenolith in Bárcena crater lava (SB4M55). H. B. Wiik, analyst.

5. Trachyandesite or mugearite (SB38M53). Pre-Montículo Cinerítico lava. H. B. Wiik, analyst.

6. Sodic trachyte (SB9M53). Bárcena crater lava. H. B. Wiik, analyst.

7. Sodic trachyte (SB25M53). Delta Lávico lava. H. B. Wiik, analyst.

8a. Sodic trachyte. Volcán Bárcena pumiceous ash (SB23M53). H. B. Wiik, analyst.

8b. Sodic trachyte. Analysis 6a computed water-free with enough Na_2O combined with Cl to give NaCl, which is excluded.

9. Sodic trachyte (SB15M53). Cráter Herrera lava. H. B. Wiik, analyst.

10a. Sodic rhyolite (sample 216). Drift pumice collected 104 miles north of Isla San Benedicto. W. H. Herdsman, analyst. (Analysis includes nil Ba and Sr.)

10b. Sodic rhyolite. Analysis 10a computed water-free with enough Na_2O combined with Cl to give NaCl, which is excluded.

11a. Sodic trachyte (rhyolite) (SB21bM55). Montículo Cinerítico pumice. H. B. Wiik, analyst.

11b. Sodic rhyolite. Analysis 11a computed water-free with enough Na_2O combined with Cl to give NaCl, which is excluded.

12. Sodic rhyolite (SB1M55). Accessory block ejecta from Volcán Bárcena. H. B. Wiik, analyst.

TABLE 5. *Alkali analyses.*[1]

	A	*B*	*C*	*D*	*E*	*F*	*G*
Na_2O	5.63	5.72 av.	6.48	6.63 av.	6.18	6.98	6.89
K_2O	2.14	2.47 av.	4.78	4.88 av.	3.83	4.58	4.57
CaO	n.d.	n.d.	n.d.	n.d.	n.d.	n.d.	n.d.
Net relative alpha counts/hour	26	20	28	33.5	32.5	30.5	32
	H	*(8a)*[2]	*I*	*J*	*K*	*(6)*[2]	*L*
Na_2O	7.35	(7.30)	7.68	3.51	4.83	(6.12)	6.92
K_2O	4.19	(4.25)	4.50	5.30	2.40	(3.20)	3.24
CaO	n.d.	(1.97)	1.06	1.70	n.d.	(3.77)	1.64
Net relative alpha counts/hour	37 av.		n.d.	36	21.5		n.d.
	M	*N*	*O*	*P*			
Na_2O	6.75	7.23 av.	6.81	7.07			
K_2O	3.47	3.27 av.	3.30	4.74			
CaO	n.d.	1.56	n.d.	n.d.			
Net relative alpha counts/hour	20	14	25 av.	63			

A. Trachyandesite, Punta Ortolan, dike on northeast side, SB17N53.
B. Trachyandesite, pre-Montículo Cinerítico lava, flow at west end of Volteadura Beach, SB11N53 (same as SB38M53, analysis 5 in table 4).
C. Trachyte, Cerro López de Villalobos lava, north end, SB21N53.
D. Trachyte, Montículo Cinerítico lava, east side, T947.
E. Trachyte, Cráter Herrera, north top, SB15N53.
F. Trachyte, Cráter Herrera, south side, SB16M53.
G. Trachyte, Roca Challenger, north side, SB13M53.
H. Trachyte, Volcán Bárcena pumiceous ash, SB23M53.
I. Trachyte, Bárcena pumice, SB21M53.
J. Trachyte, Bárcena glassy ejecta, SB22M53.
K. Trachyte, Bárcena crater lava, SB9M53.
L. Trachyte, Bárcena crater lava (more vitric than SB9M53), SB8M53.
M. Trachyte, Delta Lávico lava, first flow, SB3D52.
N. Trachyte, Delta Lávico lava, north end of flow, SB26M53.
O. Trachyte, Delta Lávico lava, from mouth of vent, last flow, SB3N53.
P. Sodic rhyolite, Bárcena accessory block ejecta, SB19N53.

[1] Analytical methods and procedure for obtaining alpha counts are described by Adams (1954, p. 90-92). The CaO analyses were made using a wet chemical method.

[2] Value from chemical analysis (table 4) listed for comparison.

in a groundmass of laths and microlites of oligoclase (An_{25}). Pale tan to green augite (+2V 55°, Z∧c 50°), while rare as megaphenocrysts, occurs as subhedral laths and prisms commonly 0.5 mm. long. They are sometimes zoned, apparently with a slightly higher sodic content (greener color) in the rim. Aegirine-bearing augite (Z∧c 60°) in the groundmass is present as tiny laths or granules. Phenocrysts of olivine (about Fo_{70}) are rare. Olivine microphenocrysts in the groundmass, about 0.2 mm. in diameter are subhedral with embayed interiors and marginal resorption, some marginal alteration to opaques is present, but iddingsite was not observed. Magnetite occurs as microphenocrysts up to 0.3 mm.; it also occurs finely divided in the groundmass causing the lava to appear black in hand specimen. Glass, with an average index of refraction of 1.527, is usually present as a minor constituent of the groundmass, but may on occasion comprise one-third or more of the groundmass giving the rock a hyalopilitic texture. Apatite is rare and commonly occurs as tiny needles in alkali feldspar phenocrysts. A little interstitial quartz and a blue sodic amphibole are present in one sample from the Delta Lávico.

A specimen of the youngest lava of the delta was collected from the mouth of the vent. Sanidine is present in the thin section but plagioclase was not observed. The alkali content of this trachyte (table 5, column O) is similar to the other crater and delta lavas. A second sample, which was collected nearby, is the usual oligoclase andesite. Alkali presumably is occult in the glass but it must also be occult elsewhere when there is little glass.

Bárcena lavas are classed as sodic trachytes according to their chemical composition.

Chemical analyses of crater and delta lavas are given in table 4, nos. 6 and 7. A series of alkali analyses of crater and delta lavas is given in table 5, columns K to O.

Olivine-bearing basalt occurs as rare xenoliths, up to about 6 inches in diameter, in Bárcena lavas. In one very vesicular sample having an intergranular texture, plagioclase was zoned from about An_{55} to An_{30}. Other constituents included non-pleochroic, greenish-tan augite (+2V 50°, Z∧c 60°), anhedral olivine and a little euhedral apatite. The one sample analyzed strangely contained no water (table 4, no. 4). Although this lava is classified a basalt according to Rittmann's system, in all probability, compared to the analyses of the trachybasalts, it should be considered an alkali basalt or trachybasalt.

PETROCHEMISTRY

Twelve new chemical analyses are listed in table 4. Cation weight percentages in parentheses follow the oxide percentage column; they were obtained using conversion factors computed by Green (1955, p. 304). Analyses 8 and 11 of pumice and ash show apparent water and salt contamination, probably derived from surf spray before the samples were collected. The pumice analyzed in column 10a had floated in the ocean for several weeks before it was collected. The analysis of this pumice shows excessive absorbed water, Na_2O, and Cl. All three analyses have been computed water-free with enough Na_2O assigned to Cl to yield halite, which was excluded because igneous rocks commonly contain less than 0.05 per cent chlorine (Kuroda and Sandell, 1953, p. 884). However, Zies' (1960) recent analyses showing relatively large amount of insoluble Cl in pantellerites are suggestive that this assumption may be questionable. In column 10a a correction was not made for fluorine. While the analyzed amount is high, it is within the range of values in eruptive rocks reported by Shepherd (1940, p. 119).

In the listing of C.I.P.W. norms (table 5), summation of the calcium, magnesium, and iron metasilicates is given in preference to a breakdown into normative diopside and hypersthene because these minerals do not appear in the mode and their use might be confusing. A norm is not given for the altered exterior of the dredged trachybasalt (analysis 1a), nor is the analysis shown in the variation diagrams.

The trachybasalt dredged from North Ridge (table 4, nos. 1 and 2) keys out to be a "nephelite basanite" in Rittmann's (1952) classification. This name is not adopted because of the absence of modal feldspathoids and virtual absence of normative nepheline. The trachybasalt shows impoverishment of silica, calcium, and potassium, enrichment of magnesium and sodium, and oxidation of the ferrous iron resulting from submarine weathering. Mellis (1960) and Matthews (1962) described similar alteration in mafic rocks dredged from the Atlantic, except that an increase in silica was found by Mellis and both writers report enrichment rather than impoverishment of potassium. Correns (1937) likewise reports enrichment of potassium in a basalt dredged from the Atlantic and impoverishment of SiO_2, FeO, CaO, MgO, and Na_2O.

The trachybasalts, although unusually high in Al_2O_3 for oceanic rocks, are not high-alumina basalts because of their Na_2O and K_2O content. They are similar to alumina-rich alkali basalts occurring in Japan, Hawaii, and elsewhere that have been described and discussed by Kuno (1960).

Alkali analyses, four of which include CaO, and alpha activity of 16 samples (table 5) were obtained for me by Dr. Edward J. Zeller, previously with the University of Wisconsin. Three alkali analyses are duplicated by chemical analyses. Variability between different analyses of the same sample is within the range of values reported by Fairbairn and others (1951) and Stevens and others (1960) except for alkali analysis K, which appears to be in error. The relation between alpha activity and uranium content has been discussed by Adams (1954).

Petrology and Relation to the East Pacific Rise

Isla San Benedicto represents only a very small proportion of the total volume of the volcanic structure, the bulk of which is below sea level. When considering magmatic differentiation of the insular and offshore rocks, it must be kept in mind that these rocks represent only the top of the volcanic pile; presumably they are also the latest and most silicic differentiates.

A Harker variation diagram of the analyzed San Benedicto rocks is shown in figure 17. It is not further mentioned for reasons similar to those ably expounded by Chayes (1964b). Ionic variation diagrams of these rocks (figs. 18 and 19) show the relationship between (Fe^{+2} + Fe^{+3}), (Na + K), and Mg, and between the alkalis and calcium. Also shown in these diagrams is the ionic variation of the similar Hawaiian alkali basalt-trachyte suite after Nockolds and Allen (1954, fig. 17). There is only a small departure of points from smooth curves and the trend of differentiation at San Benedicto from trachybasalt or alkali basalt to sodic rhyolite is indicated by arrows. Fractionation of felsic minerals with alkali enrichment and improverishment of iron and Mg is dominant over fractionation of ferromagnesian minerals with attendant iron enrichment. The most mafic rocks show a rapid impoverishment in Ca and enrichment in alkali as differentiation proceeds. At the felsic end of the curves a slight enrichment of K is apparent, more so for San Benedicto than for Hawaiian rocks. Green and Poldervaart (1958, p. 95) believe that in the production of sodic versus potassic rocks the effects of locally operative processes predominate over the generally operative fractionation process, which tends to produce rocks with a Na/K ratio of unity. Ionic variation in Si, Al, and Na (fig. 20) shows that initial differentiation was an enrichment of Si and impoverishment in Al. The rapid increase in Na curiously occurs over the silica interval (53 to 57 weight per cent SiO_2) believed to constitute a compositional "gap" by Barth (1939, p. 65–66) for rocks from the Hawaiian islands, which recently has been discussed by Chayes (1963a, 1963b), Harris (1963), Macdonald (1963), Bryan (1964), and others. Figure 20 also shows the close relationship of variation in San Benedicto rocks compared to the average alkali trachyte and peralkaline rhyolite of Nockolds and Allen (1954). Rocks from Socorro and Easter Island show a similar relationship, except that a higher degree of variation in Si occurs and there is a second phase of enrichment in Na (fig. 21, A and B).

The alkali-lime index (Peacock, 1931) for San Benedicto rocks is 52.6 or alkali-calcic; for Hawaiian rocks it is about 54 (Macdonald, 1949, p. 1570).

Nockolds and Allen (1953, p. 106) believe that the mafic end of the smooth curves in their ionic variation diagrams represented the parental magma; the scatter of points beyond the smooth curves were interpretated as accumulative rocks. There are no points beyond the smooth curves shown for San Benedicto rocks (figs. 18 and 19). The parent magma at San Benedicto appears to be a more-or-less normal alkali basalt. The oceanic character of the suite of basalts is shown by the high TiO_2 content (Chayes, 1964a). This magma is not tholeiitic fig. 23), based on the rocks thus far analyzed compared to the similar Hawaiian alkali suite presented by Kuno and others (1957). In later papers by Macdonald

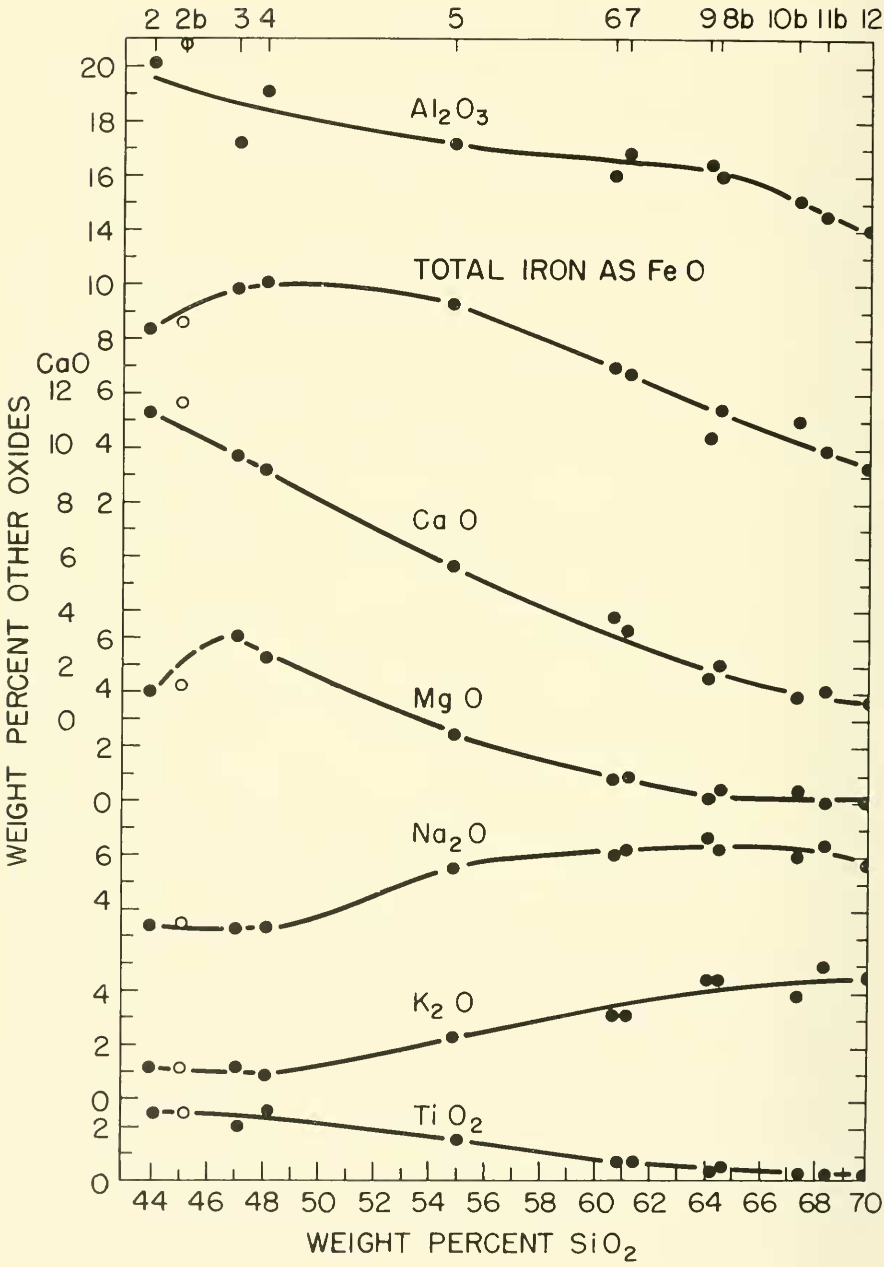

FIGURE 17. Harker variation diagram of San Benedicto rocks. The water-free sample 2b, represented by the open circles, is shown for information only.

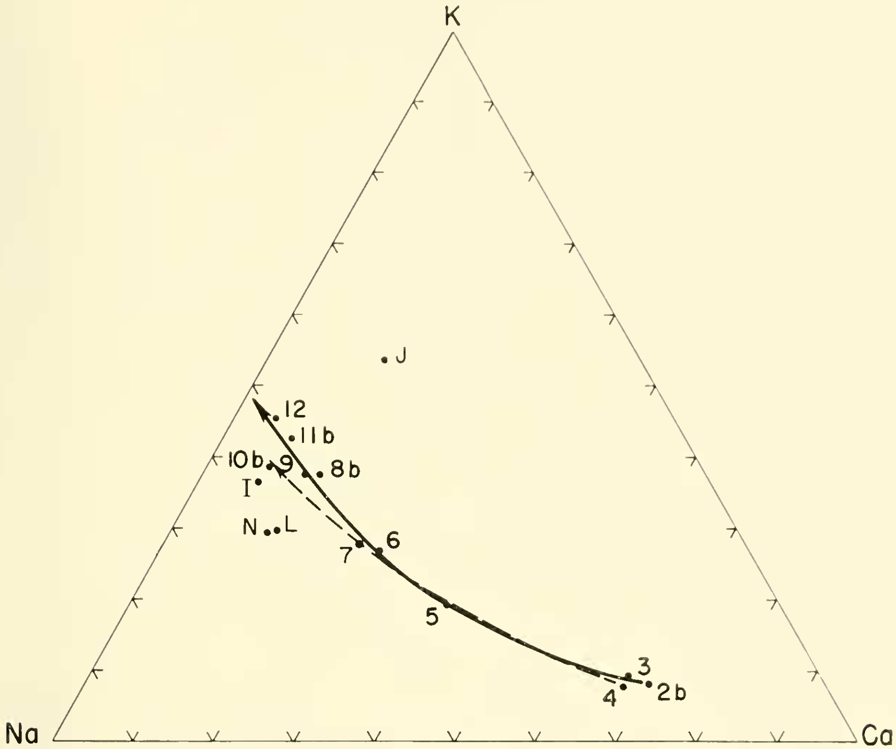

Figure 18. Ionic variation diagram of San Benedicto rocks. Variation of K – Na – Ca. Dashed line denotes variation of the Hawaiian alkali basalt-trachyte suite (Nockolds and Allen, 1954, fig. 17).

and Katsura (1962, fig. 2; 1964, fig. 1), an alkali-silica diagram illustrates the difference between tholeiitic and alkali fields. While the boundary shown in figure 22 (which was drawn in 1960) is slightly different, compared to the position of the boundary given by Macdonald and Katsura, the relationship remains unchanged.

The final stage of differentiation, from sodic trachyte to sodic rhyolite, is similar to that observed on other oceanic islands. Lavas containing at least 10 per cent modal or 15 per cent normative quartz with SiO_2 contents of about 70 per cent or more occur on the following (intrapacific) islands within the basin: San Benedicto (this paper) and Socorro (Bryan, 1959), Islas Revillagigedo; Marutea du Sud, Tuamotu Islands (Lacroix, 1927, 1939); Easter Island (Lacroix, 1936, 1939; Bandy, 1937); Oahu, Hawaii (Macdonald and Katsura, 1962; 1964); Tutuila, Samoa (Daly, 1924; Macdonald, 1944); and Hiva Oa, Marquesas (Barth, 1931). These high-silica rocks generally appear closer in composition to the average alkali or peralkali rhyolites of Nockolds (1954) than

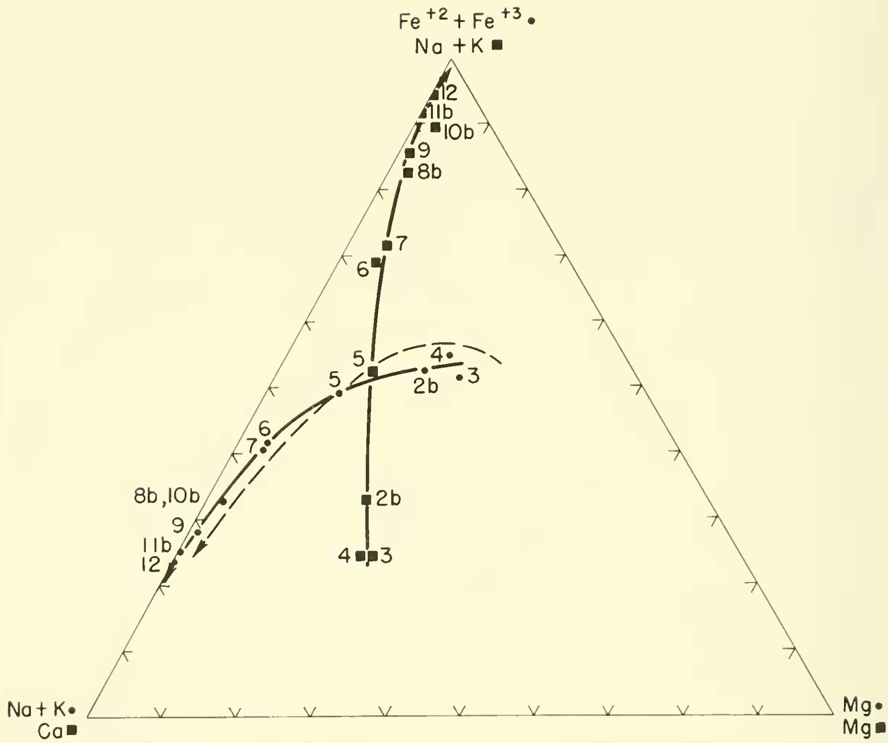

FIGURE 19. Ionic variation diagram of San Benedicto rocks. Dots show variation of total Fe – Na + K – Mg, and squares show variation of Na + K – Ca – Mg. Dashed line denotes variation of the Hawaiian alkali basalt-trachyte suite (Nockolds and Allen, 1954, fig. 17).

to his alkali or peralkali trachytes (fig. 22). All appear to be normal silicic derivitives from alkali basaltic magmas (Daly, 1925, 1934; Bandy, 1937; Tilley, 1950; Richards, 1957a; Bryan, 1959; Kuno, 1959).

It is postulated that the occurrence of the extreme silicic differentiation products (sodic rhyolite) on San Benedicto is related to the rising convective currents located under the crest of the East Pacific Rise. A discussion of the relationship of high heat flow, thin crust above the Moho, and other evidence pointing to mantle convection under the Rise has been summarized by Hess (1962) and Menard (1964).

It follows from the concept of the spreading sea floor (Hess, 1959; Dietz, 1961; Wilson, 1963a; and others) that rhyolites are not found on Roca Partida or Clarión because these islands were formed by primitive (mafic) volcanic activity occurring at an early stage in the convective process that created the East Pacific Rise. Such a process may have been similar to that proposed by Hess (1954, fig. 10, hypothesis B).

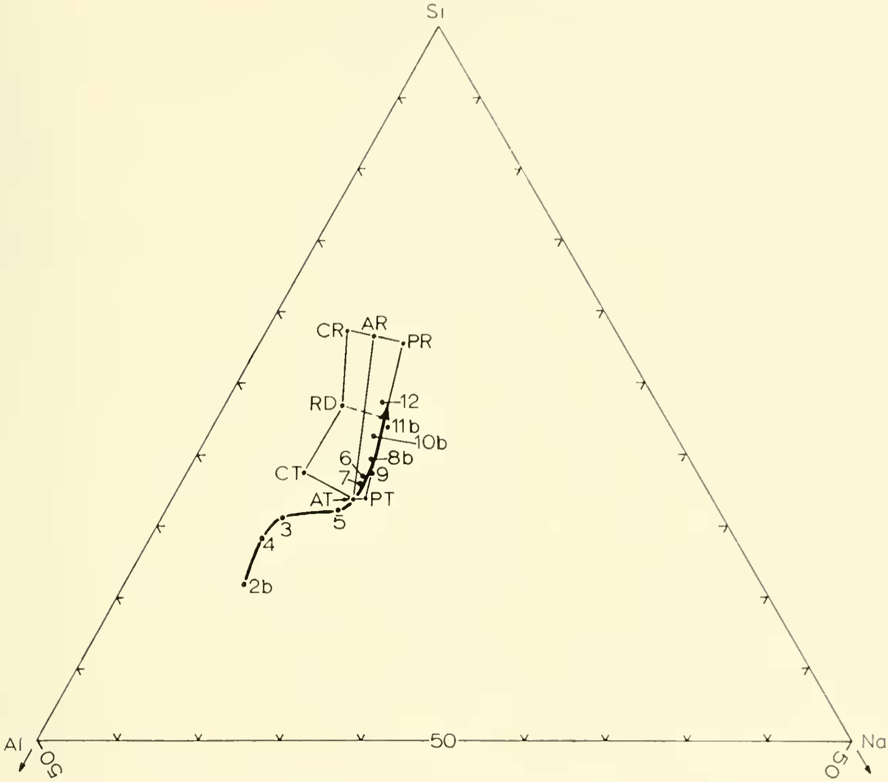

FIGURE 20. Ionic variation diagram of San Benedicto rocks showing variation of Si – Al – Na (SAN diagram). Also shown are the average: calc-alkali rhyolite and rhyolite obsidian (AR), peralkaline rhyolite and rhyolite obsidian (PR), rhyodacite and rhyodacite obsidian (RD), and the corresponding calc-alkali trachyte (CT), alkali trachyte (AT), and peralkaline trachyte (PT) that are given by Nockolds and Allen (1954). Lines connecting average values were drawn by me for illustrative purposes.

After Clarión was built above sea level by successive outpourings of relatively mafic lava, it gradually was carried along by translatory convective movement to its present position about 380 nautical miles west of the median of the crest. Wilson (1963a, 1963b, 1964) has presented evidence that "of eleven straight chains of young islands in the Pacific, ten get older away from the east Pacific rise." San Benedicto and Socorro presumably have moved less far, and increasing time somehow has enabled a higher degree of differentiation to occur, which ultimately led to the late eruption of rhyolites on these islands. Present volcanic activity attests to the fact that the process is continuing. The relationship within the suite of chemically analyzed lavas on each of the four islands is shown in figure 24.

Observed differentiation of Bárcena magma was slight. It consisted of a decrease in Si and K and an increase in most of the other elements from pumiceous ash (analysis 8b) to crater (analysis 6) and delta (analysis 7) lavas (figs. 17–20). Na remained relatively constant. The minor differences between the crater and delta lavas may not be significant.

At the beginning of the eruption the gas-rich, silicic top of the magma reservoir was erupted as ash, probably following Verhoogen's (1951) postulation. After the gas pressure had diminished, lava was later erupted from a lower level in the magma chamber. It was less silicic, somewhat richer in ferromagnesian minerals than the upper part that erupted first, and showed a fivefold reduction in water of crystallinity. The presence of olivine-bearing trachybasalt xenoliths in trachyte indicates the existence of these rocks at lower levels and thus indirectly supports the conclusion that differentiation probably resulted from the normal fractional crystallization of an alkali basalt magma.

While the silicic differentiates do not appear to be related to a tholeiitic magma, such as was suggested by Macdonald and Katsura (1964, p. 106) to account for the rhyodacite on Oahu, it is recognized that the alkali series *may be* derived from a tholeiitic magma following the line of evidence presented by Engel and Engel (1964) and Kushiro (1964). As mentioned previously, however, there appears to be no evidence for tholeiitic volcanics on San Benedicto. More convincing are the arguments (Yoder and Tilley, 1962) that tholeiitic and alkali-basalt magmas are derived from a single parent. The derivation is pressure (depth) dependent, and alkali-type basaltic liquids were considered to be produced at higher temperatures than tholeiitic liquids (p. 520). If this relation is valid at depth in the vicinity of San Benedicto, it is unlikely that tholeiitic rocks underly the volcanic pile.

Oceanic Rhyolites from Islands on the East Pacific Rise

Peterson and Goldberg (1962) reported on the relative abundances and types of feldspar in pelagic sediments of the South Pacific. Their work showed that volcanism along the crest of the East Pacific Rise produced silicic lavas, which were characterized by an abundance of locally-derived alkali feldspars, and that the proportion of more mafic lavas, containing plagioclase feldspars, increased with increasing distance away from the Rise crest. They also found a distinctly higher quartz/feldspar ratio in the coarse-size fraction of sediments collected near the crest. The relation of the Revillagigedo volcanics to the Rise had not been recognized prior to the publication of this important study.

The occasion of giving an invited paper on the petrochemistry of the East Pacific Rise at Kiel University in early 1963 provided an opportunity to reexamine the relationship in the Archipiélago de Colón (Galápagos). This group of islands trend approximately normal to the trend of the East Pacific Rise, although the situation is complicated by the presence of the Cocos Ridge, extending northeast, and the Carnegie Ridge extending east of the archipelago

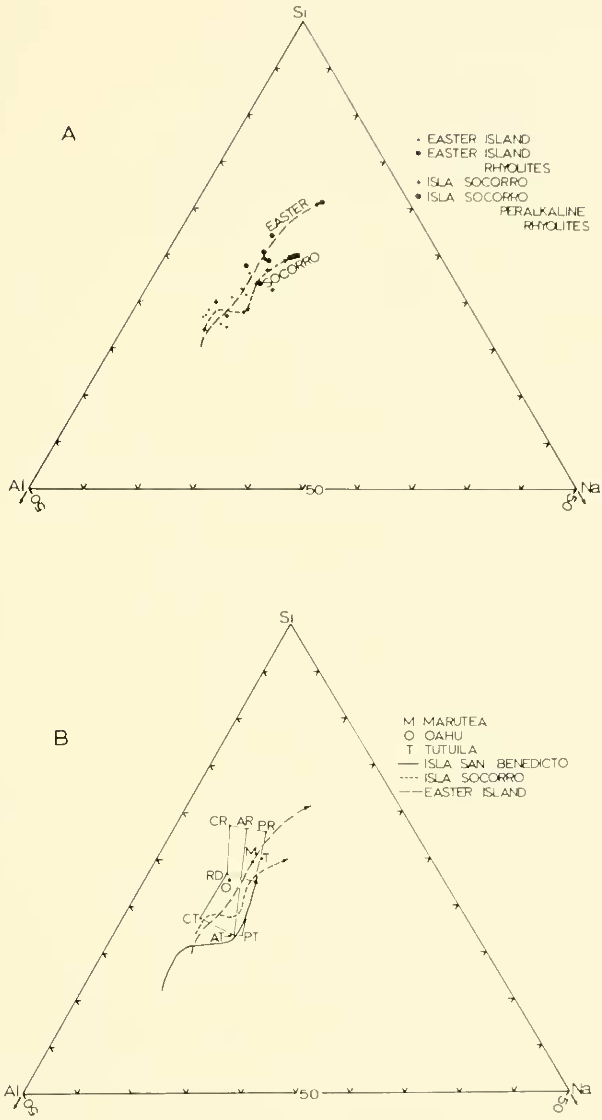

FIGURE 21. Ionic variation diagrams for oceanic rhyolites from intrapacific islands. A. SAN diagram for Easter Island (data from Lacroix, 1939, analyses 4–10, 12–19) and Isla Socorro (data from Bryan, 1959, p. 88–90). B. SAN diagram of rhyolite from Marutea (Lacroix, 1927, p. 45), rhyodacite from Oahu (Macdonald and Katsura, 1962, p. 192), and quartz trachyte from Tutuila (Daly, 1924, p. 107). Other symbols are explained in the caption to figure 20.

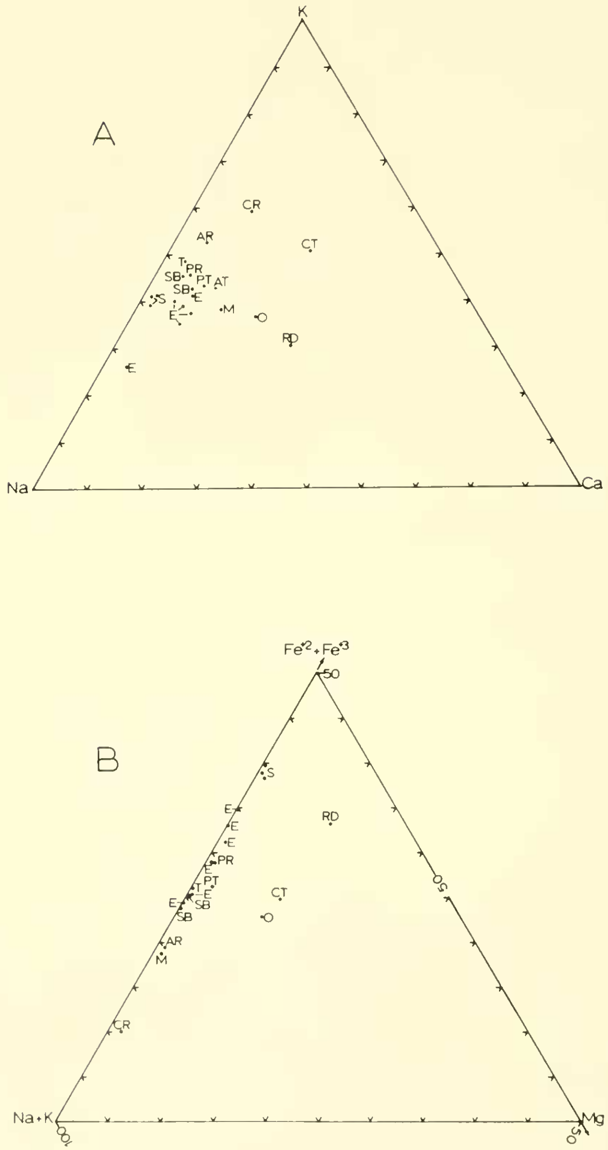

FIGURE 22. Ionic variation diagrams for oceanic rhyolites from intrapacific islands. A. Variation of K – Na – Ca. B. Variation of $Fe^{+2} + Fe^{+3}$ – Na + K – Mg (FAM diagram). In the diagrams E represents Easter Island, M the Marquesas Islands, O Oahu Island, S Isla Socorro, and SB Isla San Benedictò; other letters are explained in the caption to figure 20.

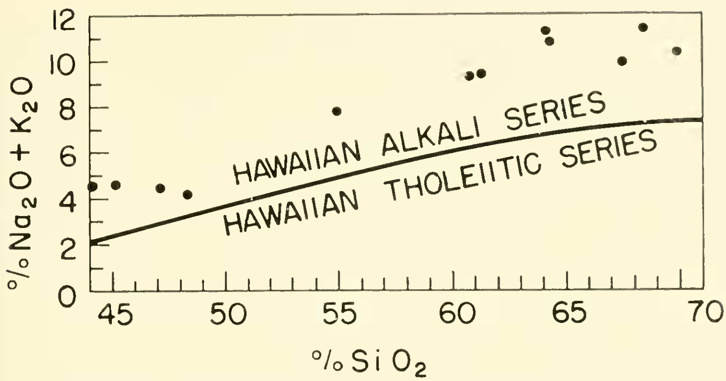

FIGURE 23. Alkali related to silica in San Benedicto rocks. The line divides the Hawaiian alkali rocks from the Hawaiian tholeiitic rocks (after Kuno and others, 1957). The position of this line also is nearly identical to a line separating the Circum-Japan alkali series and the Izu-Hakone tholeiite series reported by Kuno (1959).

(Shumway, 1954, 1957). In a recent summary of historic volcanic activity in this island group (Richards, 1962), it was shown that the most active volcanoes were confined to the extreme west end of the archipelago, which is nearest to the crest of the Rise. While insufficient evidence is available to state whether there exists an areal relationship of silicic and mafic rocks to the Rise, the islands at the eastern end of the archipelago definitely appear older than those at the western end, an observation previously stated by Chubb (1933, p. 21–22).

It probably is not a coincidence that the sodic rhyolites from Easter, Socorro, and San Benedicto are similar (figs. 21 and 22). The most silicic rhyolites found anywhere on intrapacific islands occur on Easter, which lies on the crest of the East Pacific Rise. Sodic rhyolites found on San Benedicto and Socorro, which are located west of the outer limit of the crest, are not as highly differentiated with respect to silica.

On other intrapacific islands, rhyodacite has been reported from Oahu (Macdonald and Katsura, 1962, p. 192; 1964, p. 106–107), sodic rhyolite from Hiva Oa, Marquesas Islands (Barth[4], 1931, p. 525–526), and sodic rhyolite (quartz trachyte) from Tutuila, Samoa Islands (Daly, 1924, p. 106–107; Macdonald, 1944, p. 1344–1347). None of these islands appear to be associated with a rise. All are related to fissures or fracture zones from which vast outpourings of lava have built the submarine foundations of each archipelago. Variation in selected cations is shown in figure 21.

The sodic rhyolite pumice collected from what evidently was a deposit of

[4] Barth refers to a paper, "Petrology of the Marquesas Islands," in press by H. S. Washington. The manuscript was never published and it and the analysis of this rhyolite by Keyes appear to be lost (Yoder and Tilley, 1962, p. 405; F. Chayes, 1965, personal communication).

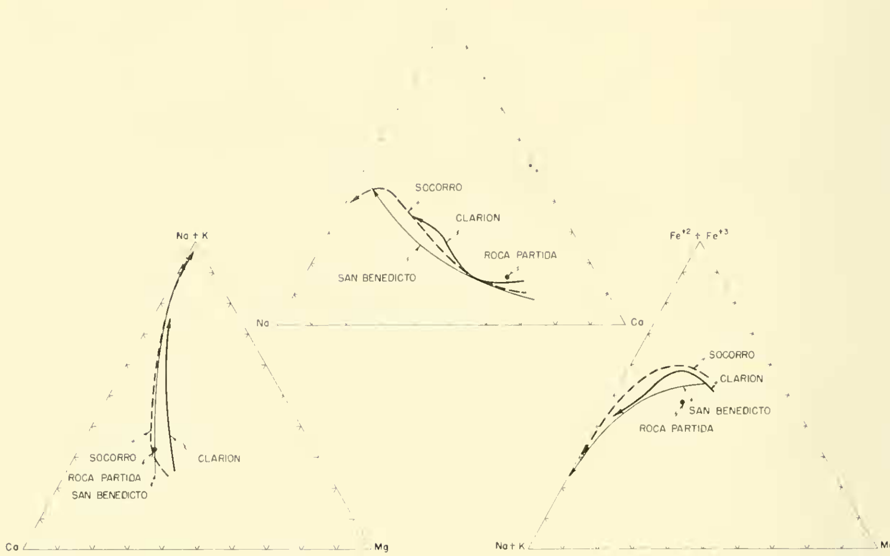

Figure 24. Ionic variation diagram for the volcanic rocks of the four Islas Revillagigedo. The arrow length represents the range of values reported. Chemical data for Isla Socorro and Isla Clarión are from Bryan (1959); for Isla Roca Partida they are from Richards (1964).

beach rock on Marutea, Tuamotu Archipelago (Lacroix, 1927, p. 44–45), probably did not originate from a volcano in the Tuamotus, where other sodic rhyolites are unknown. The similarity of the analysis of the Marutea pumice compared to the sodic rhyolites from Easter suggests that it may have drifted to Marutea in the South Equatorial Current following an eruption on Easter. An oceanic drift previously was proposed by Lacroix, who did not suggest a place of origin.

With respect to Easter, it is strange that silicic differentiates have not been reported from Sala-y-Gomez, which is located near Easter Island (Fisher and Norris, 1960) and appears to be composed of lavas of the alkali basalt suite.

It is concluded that while magmatic differentiates as silicic as sodic rhyolite occur on a few islands at or near the crest of the East Pacific Rise, there is no evidence to date indicating that other sodic rhyolites in the Pacific basin are intimately associated with rises.

SUMMARY AND CONCLUSIONS

Isla San Benedicto is located at the north end of a range of submarine volcanoes (and Isla Socorro) that comprise the Mathematician Seamounts. A more satisfactory name for this feature of north–south trending basins and ridges (Richards, unpublished) would be the San Benedicto-Clipperton Ridge.

This ridge is cut by the Clarion Fracture Zone, and its landward continuation of the trans-Mexico volcanic axis, in the latitude of San Benedicto and Socorro. A pattern of local ridges mark the presence of fissures from which have erupted the sequence of alkali basalt to sodic rhyolite that form the island and the submarine ridge that trends north of San Benedicto.

The insular shelf of San Benedicto is poorly developed; shelf-break occurs about 55–60 fathoms at the south end and 70–75 fathoms at the north end of the island. Ascending magma under the south end of the island is believed to satisfactorily account for the tilt of the shelf.

Volcanism progressed from north to south in the immediate vicinity of San Benedicto; the oldest rocks are at the north end. This volcanism probably occurred during the Pleistocene or at least during the late Cenozoic; the island is older than late Pleistocene.

The first geological map of San Benedicto shows the relations of the eroded volcanics at the north end of the island, the large trachytic domes in the center, and the two newest pyroclastic volcanoes, Montículo Cinerítico and Bárcena, at the south end. The latter volcano originated between August, 1952, and March, 1953.

Petrographic investigations and chemical studies based on 12 new analyses show a differentiation sequence:
Trachybasalt (alkali basalt) → trachyandesite (mugearite) → sodic trachyte → sodic rhyolite.

Tholeiites and high alumina basalts have not been found and are believed not to exist in the vicinity of San Benedicto. The trachyandesite appears marginal in composition between hawaiite (Macdonald, 1960) and mugearite. Evidence is presented that while the sodic rhyolites are unusual, they are considered to be normal extreme differentiates in the sequence. The described sodic rhyolites do not appear to be pantellerites.

With increasing distance from the crest of the East Pacific Rise, the geologic age of the Revillagigedo islands increase and there is a progression towards more mafic volcanics to the west. The sodic rhyolites of San Benedicto and Socorro are not found on Isla Clarión or Isla Roca Partida. Active volcanism is confined to San Benedicto and Socorro, which are nearest to the crest of the Rise.

A similar relationship is reported for the Archipiélago de Colón (Galápagos Islands); however, the active volcanoes are at the west end of the archipelago and the age of the islands increases to the east.

Elsewhere in the east Pacific possible relationships between petrographic provinces and oceanic rises generally are not clear because of the paucity of samples and the conflicting nomenclature. In the years since Macdonald's (1949) classic paper summarized volcanic rocks found on central and some east Pacific islands, igneous rocks have been collected and described from a number of east Pacific islands and submarine volcanoes by Bryan (1959), Budinger and Enbysk (1958), Carsola and Dietz (1952), Chesterman (1963), Engel and Engel (1963, 1964), Fisher and Norris (1960), Johnson (1953), Krause (1961, 1964), Obermuller (1959), and Richards (1957a, 1957b, 1958b, 1964). Little more can be said than that all of the described rocks appear to represent reasonably normal oceanic volcanics as defined by Macdonald (1960) and discussed by Chayes (1964a). Very recently, however, an increasing number of tholeiitic basalts have been dredged from the sea floor. It is likely that this trend will continue, as shown by Moore's (1965) description of dredged tholeiites from the vicinity of Hawaii.

APPENDIX

Topographic map of San Benedicto.

The following assumptions were made by me when contour interval, coordinates, and scale were established in the preparation of figures 2 and 4.

The maximum altitude of Bárcena was determined by four different methods: (1) a 1250-foot altitude was obtained from nearly identical altimeter readings made on three flights in 1952 and 1953. (2) On the May 25, 1955, flight a radio altimeter measurement indicated 1120 feet for the maximum altitude. (3) A figure of about 1130 feet was obtained by parallax measurements (Tewinkel, 1952, p. 324–328) from photographs taken in May, 1953. (4) The external slope of Bárcena is 33°. Assuming that the map scale is correct, a 1100-foot maximum altitude is indicated by trigonometry. Altimetry measurements are frequently unreliable because of differences in barometric pressure owing to the lapse of time between readings made for calibration and at the point to be determined. The latter three methods are more accurate and they indicate an approximate maximum altitude of about 1120 feet.

Twenty-one form lines are shown on the original "topographic map" made by Jack Caudry, PHC, USN. The resulting contour interval is 52 feet, based on a maximum altitude of 1090 feet for the 21st form line. Form line or contour accuracy is very good south of Cráter Herrera and fair to good north of Cráter Herrera (Jack Caudry, personal communication). Some cliffs should be steeper than indicated, particularly Roca Challenger and Cráter Herrera.

The map scale was determined photogrammetically using the relation that the natural scale is equal to the flying altitude divided by the focal length of the camera lens. This figure was verified by extrapolation from the measured lengths of Banda and Volteadura beaches made in November, 1953, by Donald Wise and James Bobcock.

True north was obtained in May, 1955, from the R/V *Crest* by gyrocompass bearings made between the Delta Lávico, Bárcena, Punta Ortolan, and Punta Observer. The reproducibility of the measurements is about one degree.

Coordinates are based on Punta Sur, which was determined by the U.S.S.

Narragansett Survey in 1874 (Dewey, 1874) to be located at 19° 17′ 15″ north latitude and 110° 49′ 25″ west longitude (U.S. Navy Hydrographic Office chart no. 1687, 9th ed., May, 1925). This position is approximate because in the late ninteenth century longitude was based on chronometer time obtained in the last port of call and it was not possible to establish precise positions from shipboard.

Bathymetry.

In the preparation of figure 5, soundings originally were plotted to a chart scale of 1:21,000; the chart, with 50-fathom contours, was pantographed to a scale of 1:49,500 before it was redrawn showing 100-fathom contours.

Soundings were taken with a Navy type NMC-1 echo sounder, calibrated for a nominal sound velocity in sea water of 4800 feet per second. They have not been corrected for velocity variation due to effects of temperature, salinity, and pressure. True depths would be about 2 per cent greater.

Control of ship position near San Benedicto was based on horizontal sextant angles, pelorus bearings from a gyrocompass repeater, and radar ranges. North of the island, where sextant angles tangent to the east and west sides were less than 5° to 7°, positions were obtained from pelorus bearings, radar ranges, and dead reckoning.

Terminology of topographic features in general conforms with definitions proposed by the International Committee on the Nomenclature of Ocean Bottom Features (Wiseman and Ovey, 1953).

REFERENCES CITED

Adams, J. A. S.

1954. Uranium and thorium contents of volcanic rocks, p. 89–98, *in* Faul, H. (Editor), Nuclear geology. New York, John Wiley, 414 pp.

Banda, L.

1862. Informe presentado al gobierno del Estado de Colima. Boletín de la Sociedad Méxicana de Geografía y Estadística, vol. 9, pp. 183–186.

Bandy, M. C.

1937. Geology and petrology of Easter Island. Bulletin of the Geological Society of America, vol. 48, pp. 1589–1610.

Barth, T. F. W.

1931. Mineralogical petrology of Pacific lavas. Pt. 2, Rocks. American Journal of Science, vol. 221, pp. 491–530.

1939. Die Eruptivgesteine, pp. 1–115 *in* Barth, T. F. W., C. W. Correns, and P. Eskola. Die Entstehung der Gesteine. Berlin. Julius Springer, 422 pp.

Bowen, N. L.

1937. A note on aenigmatite. American Mineralogist, vol. 22, pp. 139–140.

Brattstrom, B. H.

1963. Bárcena Volcano, 1952: its effects on the fauna and flora of San Benedicto Island, Mexico. Symposium "Pacific basin biogeography," 10th Pacific Science Congress, Honolulu, pp. 499–524

BRYAN, W. B., Jr.

1959. High-silica alkaline lavas of Clarion and Socorro islands Mexico——their genesis and regional significance. Unpublished Ph.D. thesis, University of Wisconsin, 164 pp.

BRYAN, W. B.

1964. Relative abundance of intermediate members of the oceanic basalt-trachyte association: evidence from Clarion and Socorro islands, Revillagigedo Islands, Mexico. Journal of Geophysical Research, vol. 69, pp. 3047–3049.

BUDINGER, T. F., and B. ENBYSK

1958. Cobb Seamount, a deep-sea feature off the Washington coast (abstract). Bulletin of the Geological Society of America, vol. 69, p. 1677.

BURNEY, J.

1803. A chronological history of the discoveries in the South Sea or Pacific Ocean. London, n.p., pt. 1, 383 pp.

CARSOLA, A. J., and R. S. DIETZ

1952. Submarine geology of two flat-topped northeast Pacific seamounts. American Journal of Science, vol. 250, pp. 481–497.

CHAYES, F.

1952. Relations between composition and indices of refraction in natural plagioclase. American Journal of Science, Bowen volume, pp. 85–105.

1963a. Relative abundance of intermediate members of the oceanic basalt-trachyte association. Journal of Geophysical Research, vol. 68, pp. 1519–1534.

1963b. Author's reply to the preceding discussions: Journal of Geophysical Research, vol. 68, pp. 5108–5109.

1964a. A petrographic distinction between Cenozoic volcanics in and around the open oceans. Journal of Geophysical Research, vol. 69, pp. 1573–1588.

1964b. Variance-covariance relations in some published Harker diagrams of volcanic suites. Journal of Petrology, vol. 5, pp. 219–237.

CHESTERMAN, C. W.

1963. Contributions to the petrography of the Galápagos, Cocos, Malpelo, Cedros, San Benito, Tres Marías, and White Friars islands. Proceedings of the California Academy of Sciences, 4th series, vol. 32, pp. 339–362.

CHUBB, L. J.

1933. Geology of Galapagos, Cocos, and Easter islands. Bernice P. Bishop Museum Bulletin 110, pp. 1–44, 65–67.

COLNETT, J.

1798. A voyage to the south Atlantic and round Cape Horn into the Pacific Ocean. London, W. Bennett, 179 pp.

CORRENS, C. W.

1937. Um- und Neubildungen am Meeresboden. Wissenschaftliche Ergebnisse der Deutschen Atlantische Expedition auf dem Forschungs- und Vermessungsschiff *Meteor* 1925–1927, vol. 3, pt. 3, pp. 287–295.

CROWE, B., and P. CROWE

1955. Heaven, hell and salt water: London, Adlard Coles, 264 pp.

CRUMP, R. M., and K. B. KETNER

1953. Feldspar optics, pp. 23–40 *in* Emmons, R. L. (Editor), Selected petrogenic relationships of plagioclase. Geological Society of America Memoir, 52, 142 pp.

DE CSERNA, Z.

1958. Notes on the tectonics of southern Mexico, pp. 523–532 *in* Habitat of oil. Tulsa, Oklahoma, American Association of Petroleum Geologists.

Daly, R. A.

1924. The geology of American Samoa. Carnegie Institute of Washington Publication 340, pp. 95–143.

1925. The geology of Ascension Island. Proceedings of the American Academy of Arts and Sciences, vol. 60, pp. 1–80.

1934. The sub-Pacific crust. Proceedings of the 5th Pacific Science Congress, Canada, vol. 3, pp. 2503–2510.

Dewey, G.

1874. Remarks on the coast of Lower California and Mexico. U. S. Hydrographic Office Publication no. 56, 60 pp.

Dietz, R. S. (edited by D. C. Kelley)

1953. Boqueron. Pacific Discovery, vol. 6, pp. 24–27.

Dietz, R. S.

1961. Continent and ocean basin evolution by spreading of the sea floor. Nature, vol. 190, pp. 854–857.

Dietz, R. S., and H. W. Menard

1951. Origin of abrupt change in slope at continental shelf margin. Bulletin of the American Association of Petroleum Geologists, vol. 35, pp. 1994–2016.

Engel, A. E. J., and C. G. Engel

1964. Igneous rocks of the East Pacific Rise. Science, vol. 146, pp. 477–485.

Engel, C. G., and A. E. J. Engel

1963. Basalts dredged from the northeastern Pacific Ocean. Science, vol. 140, pp. 1321–1324.

Fairbairn, H. W., and others

1951. A cooperative investigation of precision and accuracy in chemical, spectrochemical and modal analysis of silicate rocks. United States Geological Survey Bulletin 980, 71 pp.

Fisher, R. L., and R. M. Norris

1960. Bathymetry and geology of Sala y Gomez, southeast Pacific. Bulletin of the Geological Society of America, vol. 71, pp. 497–502.

Green, J.

1955. Conversion factors for silicate analysis. Annals of the New York Academy of Sciences, vol. 62, pp. 295–326.

Green, J., and A. Poldervaart

1958. Petrochemical fields and trends. Geochimica et Cosmochimica Acta, vol. 13, pp. 87–122.

Hamilton, E. L.

1956. Sunken islands of the Mid-Pacific mountains. Geological Society of America, Memoir 64, 97 pp.

Hanna, G D.

1926. Expedition to the Revillagigedo Islands, Mexico, in 1925. Proceedings of the California Academy of Sciences. ser. 4, vol. 15, no. 1, 113 pp.

Harris, P. G.

1963. Comments on a paper by F. Chayes, 'relative abundance of intermediate members of the oceanic basalt-trachyte association.' Journal of Geophysical Research, vol. 68, pp. 5103–5107.

Hess, H. H.

1954. Geological hypotheses and the earth's crust under the oceans. Proceedings of the Royal Society of London, ser. A, vol. 222, pp. 341–348.

1959. Nature of the great oceanic ridges (abstract), pp. 33–34, *in* International Oceanographic Congress Preprints. Washington, American Association for the Advancement of Science.

1962. History of ocean basins, pp. 599–620, *in* Petrologic studies, a volume in honor of A. F. Buddington. New York, Geological Society of America.

HUMBOLDT, A.

1811. Political essay on the kingdom of New Spain. (Translated from the original French by John Black.) London, Longman, and others, vol. 2, 483 pp.

JOHNSON, C. W.

1953. Notes on the geology of Guadalupe Island, Mexico. American Journal of Science, vol. 251, pp. 231–236.

KRAUSE, D. C.

1961. Geology of the southern California borderland west of Baja California, Mexico. Unpublished Ph.D. dissertation, University of California, San Diego, 205 pp.

1964. Lithology and sedimentation in the southern continental borderland, pp. 274–305, *in* Miller, R. L. (Editor) Papers in marine geology, Shepard commemorative volume. New York, Macmillan, 531 pp.

KUNO, H.

1959. Origin of Cenozoic petrographic provinces of Japan and surrounding areas. Bulletin Volcanologique, sér. 2, vol. 20, pp. 37–76.

1960. High-alumina basalt. Journal of Petrology, vol. 1, pp. 121–145.

KUNO, H., K. YAMASAKI, C. IIDA, and K. NAGASHIMA

1957. Differentiation of Hawaiian magmas. Japanese Journal of Geology and Geography, vol. 28, pp. 179–218.

KURODA, P. K., and E. B. SANDELL

1953. Chlorine in igneous rocks. Bulletin of the Geological Society of America, vol. 64, pp. 879–896.

KUSHIRO, I.

1964. The system diopside-forsterite-enstatite at 20 kilobars. Carnegie Institute of Washington, Year Book 63, pp. 101–108.

LACROIX, A.

1927. La constitution lithologique des îles volcaniques de la Polynésia Australe. Academie des Sciences, Paris, Mémoires, sér. 2, vol. 59, no. 2, 82 pp.

1936. Composition chimique des laves de l'île de Paques: Comptes rendus des séances de l'Academie des Sciences, Paris, vol. 202, pp. 601–605.

1939. Clipperton, Iles de Paques et Pitcairn. Annales de l'Institut Océanographique, vol. 18, pp. 289–330.

MACDONALD, G. A.

1944. Petrography of the Samoan Islands. Bulletin of the Geological Society of America, vol. 55, pp. 1333–1362.

1949. Hawaiian petrographic province. Bulletin of the Geological Society of America, vol. 60, pp. 1541–1596.

1960. Dissimilarity of continental and oceanic rock types. Journal of Petrology, vol. 1, pp. 172–177.

1963. Relative abundance of intermediate members of the oceanic basalt-trachyte association——a discussion. Journal of Geophysical Research, vol. 68, pp. 5100–5102.

MACDONALD, G. A., and T. KATSURA

1962. Relationship of petrographic suites in Hawaii, pp 187–195, *in* The crust of the Pacific basin. American Geophysical Union, Geophysical Monograph, number

6 (National Academy of Sciences–National Research Council Publication no. 1035).

1964. Chemical composition of Hawaiian lavas. Journal of Petrology, vol. 5, pp. 82–133.

MacKenzie, W. S.

1956. The orientation of the pericline twin lamellae in triclinic alkali felspars. Mineralogical Magazine, vol. 31, pp. 41–46.

MacKenzie, W. S., and J. V. Smith

1955. The alkali feldspars: I. Orthoclase microperthites: American Mineralogist, vol. 40, pp. 707–732.

Maldonado-Koerdell, M.

1958a. Recientes adelantos en geofísica y geología submarinas en las áreas del océano Pacífico próximas a México. Ciencia, vol. 18, pp. 105–113.

1958b. El Volcán Bárcena en la Isla San Benedicto, Archipiélago de las Revillagigedo (México). Ciencia, vol. 18, pp. 114–123.

Mathews, D. H.

1962. Altered lavas from the floor of the eastern north Atlantic. Nature, vol. 194, pp. 368–369.

Mellis, O.

1960. Gesteinsfragmente im roten ton des Atlantischen Ozeans. Göteborgs Kungliga Vetenskaps- och Vitterhets- Samhälles Handlingar, Sjätte Följden, ser. B, vol. 8, no. 6, 18 pp.

Menard, H. W.

1955. Deformation of the northwestern Pacific basin and the west coast of North America. Bulletin of the Geological Society of America, vol. 66, pp. 1149–1198.

1958. Development of median elevations in ocean basins. Bulletin of the Geological Society of America, vol. 69, pp. 1179–1186.

1959. Geology of the Pacific sea floor. Experientia, vol. 15, pp. 205–213.

1960. The east Pacific Rise. Science, vol. 132, pp. 1737–1746.

1964. Marine geology of the Pacific. New York, McGraw–Hill, 271 pp.

Menard, H. W., and R. L. Fisher

1958. Clipperton fracture zone in the northeastern equatorial Pacific. Journal of Geology, vol. 66, pp. 239–253.

Moore, J. G.

1965. Petrology of deep-sea basalt near Hawaii. American Journal of Science, vol. 263, pp. 40–52.

Mooser, F.

1958. Active volcanoes of Mexico, pp. 1–36 *in* Catalogue of the active volcanoes of the world including solfatara fields. Naples, International Volcanological Association, part 6, Central America.

Mooser, F., and M. Maldonado-Koerdell

1961. Pene-contemporaneous tectonics along the Mexican Pacific coast. Geofísica Internacional, vol. 1, pp. 3–20.

Muir, I. D., and C. E. Tilley

1961. Mugearites and their place in alkali igneous rock series. Journal of Geology, vol. 69, pp. 186–203.

Neumann van Padang, M.

1938. Über die unterseevulkane der erde. De Mijningenieur de Waterstaats-ingenieur, de Ingenieur in Nederlandsch-Indië, vol. 5e, pp. 85–103.

Nockolds, S. R.

1954. Average chemical compositions of some igneous rock. Bulletin of the Geological Society of America, vol. 65, pp. 1007–1032.

Nockolds, S. R., and R. Allen

1953. The geochemistry of some igneous rock series. Geochimica et Cosmochimica Acta, vol. 4, pp. 105–142.

1954. The geochemistry of some igneous rock series: Part II. Geochimica et Cosmochimica Acta, vol. 5, pp. 245–285.

Obermuller, A. G.

1959. Contribution a l'étude géologique et minérale de l'île Clipperton (Polynésie Française), pp. 47–60 *in* Recherche géologique et minérale en Polynésie Française. Paris, l'Inspection Générale des Mines et de la Géologie.

Peacock, M. A.

1931. Classification of igneous rock series. Journal of Geology, vol. 34, pp. 54–67.

Peterson, M. N. A., and E. D. Goldberg

1962. Feldspar distributions in south Pacific pelagic sediments. Journal of Geophysical Research, vol. 67, pp. 3477–3492.

Poldervaart, A.

1950. Correlation of physical properties and chemical composition in the plagioclase, olivine, and orthopyroxene series. American Mineralogist, vol. 35, pp. 1067–1079.

Revere, J. W.

1947. Naval duty in California. Oakland, Biobooks, 245 pp. (Reprint of Revere, J. W., 1849, A tour of duty in California. New York, C. S. Francis Co.)

Richards, A. F.

1957a. Geology, volcanology, and bathymetry of Isla San Benedicto, Mexico. Unpublished Ph.D. thesis, University of California, Los Angeles, 225 pp.

1957b. Geology of the Islas Revillagigedo, Mexico (abstract). Bulletin of the Geological Society of America, vol. 68, p. 1843.

1958a. Transpacific distribution of floating pumice from Isla San Benedicto, Mexico. Deep-sea Research, vol. 5, pp. 29–35.

1958b. Petrographic notes on two eastern Pacific oceanic islands and a seamount (abstract). Bulletin of the Geological Society of America, vol. 69, p. 1634.

1959. Geology of the Islas Revillagigedo, Mexico, 1. Birth and development of Volcán Bárcena, Isla San Benedicto. Bulletin Volcanologique, sér. 2, vol. 22, pp. 73–123.

1960. Rates of marine erosion of tephra and lava at Isla San Benedicto, Mexico. Proceedings of the XXI International Geological Congress, Copenhagen, vol. 10, pp. 59–64.

1962. Archipiélago de Colón, Isla San Felix and Islas Juan Fernández. Catalogue of the active volcanoes of the world including solfatara fields, part 14, Rome, International Association of Volcanology, 50 pp.

1964. Geology of the Islas Revillagigedo, Mexico, 4. Geology and petrography of Isla Roca Partida. Bulletin of the Geological Society of America, vol. 70, pp. 1157–1163.

1965. Geology of the Islas Revillagigedo, Mexico, 3. Effects of erosion on Isla San Benedicto 1952–1961 following the eruption of Volcán Bárcena. Bulletin Volcanologique, vol. 28, in press.

Richards, A. F., and B. H. Brattstrom

1959. Bibliography, cartography, discovery, and exploration of the Islas Revillagigedo. Proceedings of the California Academy of Sciences, ser. 4, vol. 29, pp. 315–360.